GRANT/AMES

IN-46

68067 C.P

P-99

FINAL TECHNICAL REPORT

to

University Affairs Office, 241-25
NASA-Ames Research Center
Moffett Field, CA 94035

For NASA Grant NSG-2010

entitled

THREE DIMENSIONAL DYNAMICAL AND CHEMICAL MODELLING OF THE UPPER ATMOSPHERE

from

Ronald G. Prinn (Principal Investigator)
Massachusetts Institute of Technology
Cambridge, MA 02139

and

Fred N. Alyea (Co-Principal Investigator)
Derek M. Cunnold (Co-Principal Investigator)
Carlos A. Cardelino (Co-Investigator)
Georgia Institute of Technology
Atlanta, GA 30332

INTRODUCTION

The principal goal of this project was to develop and utilize successively improved versions of a global 3-dimensional dynamical-chemical model of the stratospheric ozone layer. The major accomplishments are described in the following papers:

A three-dimensional dynamical-chemical model of atmospheric ozone. J. Atmos. Sci., 32, 170-194, (1975) (D. Cunnold, F. Alyea, N. Phillips, R. Prinn).

Stratospheric ozone destruction by aircraft-induced NO_x. Science, 188, 117-121, (1975) (F. Alyea, D. Cunnold, R. Prinn).

Stratospheric distributions of odd nitrogen and odd hydrogen in a two-dimensional model. J. Geophys. Res., 80, 4997-5004, (1975) (R. Prinn, F. Alyea, D. Cunnold).

The impact of stratospheric variability on measurement programs for minor constituents. Bull. Amer. Met. Soc., 57, 686-699, (1976) (R. Prinn, F. Alyea, D. Cunnold).

The dependence of ozone depletion on the latitude and altitude of injection of nitrogen oxides by supersonic aircraft. Amer. Inst. Aero. and Astro. Journal, 15, 337-345, (1977) (D. Cunnold, F. Alyea, R. Prinn).

On the radiative damping of atmospheric waves. J. Atmos. Sci., 34, 1386-1401, (1977) (R. Prinn).

Photochemistry and dynamics of the ozone layer. Annual Rev. Earth Plan. Sci., 6, 143-174, (1978) (R. Prinn, F. Alyea, D. Cunnold).

Preliminary calculations concerning the maintenance of the zonal mean ozone distribution in the Northern Hemisphere. Pure and Applied Geophys., 118, 329-354, (1980) (D. Cunnold, F. Alyea, R. Prinn).

The above papers described a "6-wave" version of our 3D model. Over the past several years we have also been developing a very much improved "18-wave" version. The major differences between the 18-wave and 6-wave models are a follows:

(a) Uses a horizontal diffusion coefficient, A_H, to close off the stratospheric jets.

(b) Non-zonal tropospheric forcing in the tropics (i.e., the annual or even components) has been neglected. Zonal heating terms have been reevaluated and modified slightly in the troposphere, primarily in the $P_2^0(\mu)$ component.

(c) The h profile has been modified in the troposphere to be in closer agreement with Trenberth. This has the effect of putting the non-zonal forcing at slightly higher altitudes and of increasing the rate of dissipation of available potential energy in the troposphere relative to some 6 wave computations (but not run 12).

(d) The coefficient of surface friction has been increased from 1.6 to 2.

(e) The static stability has been returned to its "original" value in the troposphere. This profile was not used in any reported 6 wave run and is more stable than that used in either run 12 or 17. The global mean temperature has also been increased by a few degrees at levels 24, 25 and 26.

(f) The vertical diffusion coefficient is set to 100 cm^2/sec throughout the stratosphere.

(g) The non-linear Jacobian terms in the model are now evaluated using transform methods rather than the original interaction coefficient technique.

This 18-wave model has now been completed and is described fully in the following pages.

AN ENHANCED DYNAMICAL/CHEMICAL MODEL OF ATMOSPHERIC OZONE

by

Dr. Fred N. Alyea, Dr. Derek M. Cunnold
and Carlos A. Cardelino

School of Geophysical Sciences
Georgia Institute of Technology
Atlanta, Georgia 30332

July 1985

TABLE OF CONTENTS

TABLES AND FIGURES

1. Basic dynamical equations and coordinate system.

The horizontal coordinate system will be longitude (positive eastward) and latitude, denoted by λ and ϕ. This dependence will be represented in spherical surface harmonics, except that certain terms, such as part of the heating and photochemistry will be evaluated point-wise at selected values of λ and ϕ. In the vertical direction pressure (p) will be used as a coordinate with finite-differences being employed. These pressure levels will be distributed at equal intervals of log P in order to give roughly equal intervals in height. We define

$$\left.\begin{aligned} P &= p \div (100 \text{ cbar}) \\ Z &= -\ell n P,\ P = e^{-Z} \end{aligned}\right\} . \tag{1.1}$$

From the hydrostatic relation $dp = -\rho g dz$ and $\rho = p/RT$, we have

$$dZ = -\frac{dp}{p} = \frac{g}{RT} dz \tag{1.2}$$

The vertical levels will be separated by a uniform value of ΔZ. To the extent that the temperature T is approximately uniform at near surface values, a change of one in Z corresponds to a height change of the order of 7 km. The bottom of the atmosphere will, for simplicity, be taken at Z = 0, i.e., at p = 100 cb instead of at the conventional sea-level pressure of 101.325 cb. The top of the "atmosphere" will be artificially set at $Z = Z_{top}$ corresponding to a geometric height of about 70 km.

The dynamical system not only assumes hydrostatic balance, but also a "quasi-geostrophic balance" in the horizontal equations of motion. Because we must consider global processes over the entire sphere, this balance must allow for complete variability of the coriolis parameter f:

$$f = 2\Omega \sin\phi$$
$$\Omega = 7.292 \times 10^{-5} \text{ rad sec}^{-1} \tag{1.3}$$

The quasi-geostrophic balance in question is obtained as follows (Lorenz, Tellus, 1960, P. 364). First, we divide the horizontal velocity $\vec{v}$ into a non-divergent part $\hat{k} \times \nabla\psi$ given by a stream function ψ and a divergent part $-\nabla\chi$, given by a velocity potential χ:

$$\vec{v} = \hat{k} \times \nabla\psi - \nabla\chi \tag{1.4}$$

If the eastward and northward components of $\vec{v}$ are represented by u and v and a is the radius of the earth, this is equivalent to

$$\left.\begin{aligned} u = a\cos\phi\frac{d\lambda}{dt} &= -\frac{1}{a}\frac{\partial\psi}{\partial\phi} - \frac{1}{a\cos\phi}\frac{\partial\chi}{\partial\lambda} \\ v = a\frac{d\phi}{d\tau} &= \frac{1}{a\cos\phi}\frac{\partial\psi}{\partial\lambda} - \frac{1}{a}\frac{\partial\chi}{\partial\phi} \end{aligned}\right\}. \tag{1.5}$$

The vertical component of relative vorticity, ζ, and the horizontal divergence of $\vec{v}$ are related to ψ and χ by

$$\zeta = \hat{k} \cdot \text{curl } \vec{v} = \nabla^2\psi; \quad \text{div } \vec{v} = -\nabla^2\chi \tag{1.6}$$

where ∇^2 is the horizontal Laplacian operator on the sphere.

The condition of the quasi-geostrophic balance is

$$\nabla \cdot f\nabla\psi = g\nabla^2 z \tag{1.7}$$

where g is gravity and z is the height of a constant pressure surface. [Unless noted otherwise, all partial derivatives with respect to λ, ϕ, and t (time) are

carried out at constant pressure (or Z)]. The hydrostatic relation,

$$g\frac{\partial z}{\partial p} = -\frac{1}{\rho} = -\frac{RT}{p} \tag{1.8a}$$

or

$$g\frac{\partial z}{\partial Z} = RT \tag{1.8b}$$

enables (1.7) to be rewritten as

$$\nabla \cdot f\nabla\frac{\partial \psi}{\partial Z} = \nabla^2 RT \tag{1.9}$$

Associated with this relation (which is a simplified form of the equation obtained by taking the horizontal divergence of the equations of motion) is the "vorticity equation":

$$\nabla^2\frac{\partial \psi}{\partial t} = -\hat{k} \times \nabla\psi \cdot \nabla (f+\nabla^2\psi) + \nabla \cdot f\nabla\chi + \nabla \cdot (\vec{F}x\hat{k});$$
$$\vec{F} = \vec{F}_r + \vec{F}_D \tag{1.10}$$

in which $\vec{F}$ represents the total dissipation forces, $\vec{F}_r$ is the horizontal frictional stress force per unit mass, and $\vec{F}_D$ is the horizontal diffusion.

The continuity equation (conservation of mass) is

$$\frac{\partial}{\partial p}\left(\frac{dp}{dt}\right) = \frac{\partial}{\partial P}\left(\frac{dP}{dt}\right) = -\nabla \cdot \vec{v} = \nabla^2\chi \tag{1.11}$$

The upper boundary condition at $Z = Z_{top}$ will be that dp/dt vanishes there. Let us define

$$X = -\int_{P_{top}}^{P} \chi dp, \quad \chi = -\frac{\partial X}{\partial P} \tag{1.12}$$

Equation (1.10) can then be rewritten as

$$\nabla^2 \frac{\partial \psi}{\partial t} = - \hat{k} \times \nabla\psi \cdot \nabla(f+\nabla^2\psi) - \nabla \cdot f\nabla\left(\frac{\partial \chi}{\partial P}\right) + \nabla \cdot (\vec{F} x \hat{k}) \qquad (1.13)$$

If we use $Z = -\ell n P$ as the vertical coordinate, the appropriate vertical advection velocity is

$$W = \frac{dZ}{dt} = - \frac{1}{P} \frac{dP}{dt} \qquad (1.14)$$

The continuity equation (1.11) in terms of W is:

$$\nabla \cdot P\vec{V} + \partial(PW)/\partial Z = 0 \qquad (1.15)$$

From (1.11), (1.12) and (1.14) we get $\partial [PW - \nabla^2 \chi]/\partial P = 0$, or

$$PW = \nabla^2 \chi \qquad (1.16)$$

Boundary conditions on W are that W vanishes at Z_{top} and that it is given by orographic upslope motion at the bottom:

$$\begin{aligned} Z = Z_{top}&: W = 0 \\ Z = 0&: W \approx \frac{\rho g w}{p} = \frac{1}{H_0} \vec{v}_4 \cdot \nabla h \end{aligned} \qquad (1.17)$$

where h is the orography and $\vec{v}_4$ is $k x \nabla\psi$ at the first interior level for ψ. Here

$$H_0 = \frac{RT_0}{g} = 7 \text{ km} \qquad (1.18)$$

is a constant.

Friction will be represented by a vertical Austausch, $\vec{Fr} = \frac{1}{\rho} \partial\vec{\tau}/\partial z = -g\partial\vec{\tau}/\partial p$. Thus $\nabla \cdot \vec{F} r x \hat{k} = \frac{\partial}{\partial P} [\nabla \cdot (\frac{-g\vec{\tau}}{P_0} x \hat{k})]$. <u>In the interior regions</u> of the model (but not at the ground), in terms of a vertical momentum diffusion coefficient, K_m, we set $\vec{\tau} = \rho K_m \partial(\hat{k} x \nabla\psi)/\partial z$, giving

$$\nabla\cdot\left(\frac{-g\vec{\tau}}{p_0}x\hat{k}\right) = \nabla\cdot\left[\frac{g^2\rho^2}{p_0^2}K_m\frac{\partial\nabla\psi}{\partial p}\right]$$

Replacing ρ by p/RT and replacing g/RT by $1/H_0$ we get

$$\nabla\cdot\left[\frac{-g\vec{\tau}}{p_0}x\hat{k}\right] = -\frac{K_m}{H_0^2}P\frac{\partial\nabla^2\psi}{\partial Z}$$

At the ground, we can set $\vec{\tau}$ equal to $0.003\,\rho_0|\vec{\bar{v}}|\vec{v}$, with $|\vec{\bar{v}}|$ a suitable mean anemometer speed (5 m/sec^{-1}) and the anemometer vector wind $\vec{v}$ equal to a rotated (α = 22.5 degrees) fraction (0.5) of $\hat{k}x\nabla\psi$ at the lowest interior level at which ψ is defined

$$\left.\begin{aligned}\vec{\tau}_{grnd} &= [0.003\bar{\rho}|\vec{\bar{v}}|(0.5)][\cos\alpha\,\hat{k}x\nabla\psi - \sin\alpha\,\nabla\psi]_{interior}\\ \nabla\cdot\left[-\frac{g\vec{\tau}}{\rho_0}x\hat{k}\right]_{grnd} &= -\left\{\frac{1}{H_0}[.003|\vec{\bar{v}}|(0.5)\cos\alpha]\right\}\nabla^2\psi_{interior}\end{aligned}\right\} \quad (1.19)$$

For H_0 = 7 km, $|\vec{\bar{v}}|$ = 5m sec^{-1} and cos α = 0.925, the coefficient here has the value 10^{-6} sec^{-1}.

The conventional quasi-geostrophic Taylor-Ekman theory (Charney and Eliassen, Tellus, 1949, Vol. 1, No. 2, P.38) gives a corresponding term ("Ekman pumping") of

$$-\left\{\frac{1}{H_0}\frac{K_m f}{2}\sin 2\alpha\right\}\nabla^2\psi \quad (1.20)$$

For $K_m = 6.2\times10^4$ cm^{2}sec^{-1} and $f = 10^{-4}$sec^{-1}, the coefficient in this derivation is 2.0×10^{-6}sec^{-1}. To summarize the horizontal friction stress term, we can write

$$\left.\begin{aligned} \nabla\cdot\vec{F}r\times\hat{k} &= \frac{\partial}{\partial P}(PF_r) \\ Z>0:\ F_r &= -\frac{K_m}{H_o^2} P \frac{\partial\nabla^2\psi}{\partial Z} \\ Z=0:\ F_r &= -k_D\nabla^2\psi_{int} \end{aligned}\right\} \qquad (1.21)$$

where k_D refers to the "surface drag coefficient" in (1.19) or (1.20). At $Z = Z_{top}$, F will vanish (no stress).

We want to note here that the pressure dependence of K_m as used in our model is the same as for K_D, the coefficient of vertical diffusivity of ozone, to be introduced later. We, thus, defer discussion of K_m and K_D values to the subsection entitled "Diffusivity for Ozone" but the results can be seen in Table 2.2.

Horizontal diffusion in the model is primarily introduced at the upper (mesospheric) levels to account for possible affects of large scale horizontal transportation resulting from energy supplied by gravity wave propagating from below. Parameterzation is accomplished through introduction of a coefficient of horizontal momentum diffusion, A_H, such that

$$\vec{F}_D = A_H\nabla^2\hat{v} \qquad (1.21.1)$$

where then

$$\nabla\cdot(\vec{F}_D\times\hat{k}) = A_H\hat{k}\cdot\nabla\times\nabla^2\hat{v} = A_H[\nabla^4\psi + \frac{2\nabla^2\psi}{a^2}] \ . \qquad (1.21.2)$$

Here "a" denotes the earth's radius and all differential operators are assumed to be in the spherical surface. In our parameterization, A_H will be a function of pressure only and will serve as the diffusion coefficient for momentum, temperature and ozone. Again, discussion of the values to be associated with A_H will be deferred to the subsection on "Diffusivity of Ozone."

The next physical statement is the thermodynamic law d (entropy) /dt = rate of heating ÷ temperature. For our perfect gas system this would be

$$C_p \frac{d}{dt}[\ell n(Tp^{-\kappa})] = \frac{q}{T} \; ; \; \kappa = \frac{R}{C_p} = \frac{2}{7} \tag{1.22}$$

where q is the rate of heating per unit mass and T the temperature. In terms of T, this becomes

$$\frac{\partial T}{\partial t} = -(\hat{k}x\nabla\psi - \nabla\chi) \cdot \nabla T - W\frac{\partial T}{\partial Z} - \kappa WT + A_H\nabla^2 T + \frac{q}{C_p} \tag{1.23}$$

in which the term $A_H\nabla^2 T$ represents the horizontal subgrid seal diffusion of temperature. We will, however, use a simplified form of this, obtained by ignoring $\nabla\psi\cdot\nabla T$ and by replacing T in $W\partial T/\partial Z$ and κWT by $\overline{T}$, where $\overline{T}$ is the horizontal average:

$$\left.\begin{aligned} T &= \overline{T}(p,t) + T'(\lambda,\phi,p,t) \\ \overline{T} &= \frac{1}{4\pi a^2}\int_{-\pi/2}^{\pi/2}\cos\phi d\phi \int_0^{2\pi} T d\lambda; \; \overline{T'} = 0 \end{aligned}\right\} \tag{1.24}$$

[This definition of $\overline{(\;)}$ and $(\;)'$ will be applicable to any variable.] This greatly simplifies the computations, and is reasonably accurate because $\nabla\psi >> \nabla\chi$ and $\partial T'/\partial Z + \kappa T'$ is generally small compared to $\partial\overline{T}/\partial Z + \kappa\overline{T}$. The result is

$$\frac{\partial T}{\partial t} = -\hat{k}x\nabla\psi \cdot \nabla T - W\left(\frac{d\overline{T}}{dZ} + \kappa\overline{T}\right) + A_H\nabla^2 T + q/C_p \tag{1.25}$$

However, this simplification has the result that we can no longer interpret (1.25) as forecasting $\overline{T}$, the horizontally averaged T; this is because the horizontal average of (1.25) gives simply

$$\frac{\partial \overline{T}}{\partial t} = \overline{q}/C_p$$

whereas the horizontal average of the exact equation (1.23) gives

$$\frac{\partial \overline{T}}{\partial t} = \frac{\overline{q}}{C_p} - \kappa \overline{W'T'} - \frac{1}{P}\frac{\partial}{\partial Z}(P\overline{W'T'}), \tag{1.26}$$

showing the effect of vertical transports of entropy by the motion. We expect little change in $\overline{T}$ from the observed annual average $\overline{T}(Z)$, however, either with season or with changes in the ozone chemistry. [The effect of the latter will be discussed separately.]

In passing, we note that

$$\left.\begin{aligned} \frac{\partial T}{\partial Z} + \kappa T &= \frac{RT}{g}\left(\frac{\partial T}{\partial z} + \frac{g}{C_p}\right) \\ &= T\frac{\partial}{\partial Z}\left[\ell n(Tp^{-\kappa})\right] \\ &= \frac{N^2}{R}\left(\frac{RT}{g}\right)^2 \end{aligned}\right\} \tag{1.27}$$

where N is the buoyancy frequency.

Finally, we describe the basic form of the equation for the (number density) mixing ratio of a trace substance such as O_3. Define

$$\chi_i = n_i \div n_m \tag{1.28}$$

where n_i is the number density of the i-th trace substance, n_m is the total number density, assumed to be equivalent to the "normal" constituents N_2, O_2 and CO_2 since n_i is very small.

$$n_m \cong p/kT \qquad (1.29)$$

k = Boltzman constant = 1.380×10^{-26} kilojoules deg^{-1}

The equation for $d\chi_i/dt$ (the rate of change following the motion) is

$$\frac{d\chi_i}{dt} = \frac{\partial \chi_i}{\partial t} + (\hat{k} \times \nabla\psi - \nabla\chi) \cdot \nabla\chi_i + W\frac{\partial \chi_i}{\partial Z}$$

$$= \frac{1}{n_m}\left(\frac{dn_i}{dt}\right)_c + \frac{1}{p}\frac{\partial}{\partial z}\left(\rho K_d \frac{\partial \chi_i}{\partial z}\right) + A_H \nabla^2 \chi_i$$

where $(dn_i dt)_c$ is the net rate of local photochemical generation of the substance (number per unit volume per unit time) and K_d and A_H are the vertical and horizontal eddy-diffusion coefficients [with dimensions $(\text{length})^2 \div \text{time}$], respectively. K_d and A_H will vary only with P.

The vertical diffusion term can be rewritten by using the hydrostatic equation as

$$\frac{\partial}{\partial P}\left[K_d\left(\frac{gP}{RT}\right)^2 \frac{\partial \chi_i}{\partial P}\right] \approx \frac{\partial}{\partial P}\left[-\frac{K_d}{H_o^2} P \frac{\partial \chi_i}{\partial Z}\right] \qquad (1.30)$$

where we have again absorbed the variation of density with T into H_o on the recognition that K_d itself is not a precisely known quantity. K_d (and the

momentum Austausch K_m) will be prescribed functions of P. The equation for χ_i is now

$$\frac{\partial \chi_i}{\partial t} = -(\hat{k}x\nabla\psi - \nabla\chi) \cdot \nabla\chi_i - W\frac{\partial \chi_i}{\partial Z} + \frac{1}{n_m}\left(\frac{dn_i}{dt}\right)_c + \frac{\partial}{\partial P}\left[-\frac{K_d}{H_0^2} P \frac{\partial \chi_i}{\partial Z}\right] + A_H\nabla^2\chi_i \quad (1.31)$$

or

$$\frac{\partial \chi_i}{\partial t} = -\frac{1}{P}\left[\nabla\cdot(P\vec{v}\chi_i) + \frac{\partial(PW\chi_i)}{\partial z}\right] + \frac{1}{n_m}\left(\frac{dn_i}{dt}\right)_c + \frac{\partial}{\partial P}\left[-\frac{K_d}{H_0^2} P \frac{\partial \chi_i}{\partial Z}\right] + A_H\nabla^2\chi_i \quad (1.32)$$

[having made use of (1.4) and (1.15) to obtain the last form].

The rate of change of $\overline{\chi}_i$ (the horizontal average) is obtained from the horizontal average of (1.32):

$$\frac{\partial \overline{\chi}_i}{\partial t} = \frac{\partial}{\partial P}\left[P\ \overline{W'\chi_i'}\right] + \left[\overline{\frac{1}{n_m}\left(\frac{dn_i}{dt}\right)_c}\right] + \frac{\partial}{\partial P}\left[-\frac{K_d}{H_0^2} P \frac{\partial \overline{\chi}_i}{\partial Z}\right] \quad (1.33)$$

The rate of change of χ_i' will, however, be obtained from a simplified form of (1.31), much as was done in the thermodynamic equation (1.25):

$$\frac{\partial \chi_i'}{\partial t} = -\hat{k}x\nabla\psi \cdot \nabla\chi_i' - W\frac{\partial \overline{\chi}_i}{\partial Z} + \left[\frac{1}{n_m}\frac{dn_i}{dt}\right]_c' + \frac{\partial}{\partial P}\left[-\frac{K_d}{H_0^2} P \frac{\partial \chi_i'}{\partial Z}\right] + A_H\nabla^2\chi_i' \quad (1.34)$$

In contrast to $\overline{T}$, where we are for the most part content to take $\overline{T}$ as given, we must predict $\overline{\chi}_i$ as well as χ_i'. Equation (1.33) will therefore be used as well as (1.34).

Presumably (1.33) need not be applied every time step in the numerical integration, $\bar{\chi}_i$ being a slowly changing function of time. However, the term $\overline{W'\chi_i'}$ must be put equal to zero at P = 1 to ensure no net creation of χ_i by the large scale motion.

The form of $(d\chi_i/dt)_c$ is discussed later. However, a special treatment must be used for the lower boundary condition on the vertical eddy flux. For the case of ozone, Galbally (Quart. J. Roy. Meteor. Soc., 1971, P. 18) shows that in the very lowest layer the vertical flux (over land) is proportional to the ground concentration

$$K_d \frac{\partial \chi}{\partial z} \approx \frac{K_d}{H_0} \frac{\partial \chi}{\partial Z} = d\, \chi_{grnd} \tag{1.35}$$

(the surface destruction of ozone being proportional to O_3). The coefficient d has a value of about 1 cm sec^{-1}. We will apply this formulation to the lowest layer in our model ($0 \leq Z \leq \Delta Z$). Values of χ are defined at the top of the layer ($Z = \Delta Z$, $j = J-1$) and at the ground ($Z = 0$, $j = J$). Thus (dropping the i-subscript on χ),

$$\left(\frac{K_d}{H_0} \frac{\partial \chi}{\partial Z}\right)_{J-1/2} = \left(\frac{K_d}{H_0 \Delta Z}\right)_{J-1/2} (\chi_{J-1} - \chi_J) = d\, \chi_J \tag{1.36}$$

whence

$$\chi_J = \chi_{J-1} \div \left[1 + \frac{d\, H_0 \Delta Z}{K_d}\right]_{J-1/2} \tag{1.37}$$

and

$$\left(\frac{K_d}{H_0 \Delta Z}\right)_{J-1/2} (\chi_{J-1} - \chi_J) = \frac{d\,\chi_{J-1}}{1 + (d\,H_0 \Delta Z / K_d} \qquad (1.38)$$

Galbally cites values of the vertical number flux of ozone molecules over land in the range 1 to 6×10^{11} mol cm^{-2} sec^{-1}. Aldaz (J. Geo. Res., 1969, P. 6943) estimates a global average of 1 to 1.7×10^{11} mol cm^{-2} sec^{-1}. Picking a representative value of 2×10^{11} mol cm^{-2} sec^{-1} and equating this to $n_m K\, \partial\chi/\partial z$, we find, for $n_m = 4.55 \times 10^{19}$ cm^{-3} and $K = 10^5$ cm^2 sec^{-1}, that a vertical gradient of ozone number mixing ratio of

$$\frac{\partial \chi}{\partial z} \sim 0.5 \times 10^{-13}\ cm^{-1} = \frac{5 \times 10^{-8}}{10\ km} \qquad (1.39)$$

is required. Galbally's data show a typical ground value for χ of $5 \times 10^{11} \div 4.5 \times 10^{19} \sim 10^{-8}$. The typical inferred downward flux of ozone observed near the ground is compatible then with a tropospheric K of 10^5 cm^2 sec^{-1} and a tropopause (10 km) value for χ of 6×10^{-8} or a 10-km value for NO_3 of $(6 \times 10^{-8}) \times (8 \times 10^{18}) \sim 50 \times 10^{10}$ cm^{-3}. This value is not greatly inconsistent with values of 10^{12} cm^{-3} which seem characteristic of the tropopause level in the meridional cross section prepared by D. Wu from the data of Hering and Borden (1967).

A special treatment of the minor species equation will be necessary at certain levels. As an example, Lindzen and Goody (J. Atmos. Sci., 1965, P. 341) show that the photodissociation of ozone is extremely rapid at heights above ~ 45 km, with a time constant becoming less than 1 hour. (They presumably use typical values of incident solar radiation). The conventional methods of "time-stepping) equations such as (1.34) require a computational time step no longer than the characteristic physical times associated with terms on the right side of (1.34). Since the advective time scale is of the order of an hour or so, we

must consider replacing (1.33) and (1.34) at these levels by the equilibrium condition.

$$\chi_i = (\chi_i)_{equil} \iff \frac{dn_i}{dt} = 0 \tag{1.40}$$

For use in radiation computations, we need N_i, the number of molecules of χ_i in the vertical column of unit cross section above a given pressure surface:

$$N_i = \int_z^\infty n_i dz = \int_z^\infty \chi_i n_m dz = \int_z^\infty \chi_i \frac{R}{k} p dz$$

$$= \frac{Rp_o}{gk} \int_o^P \chi_i dp$$

where $R = 287$ kj ton^{-1} deg^{-1} is the gas constant for air.
This gives numerically

$$N_i = 2.12 \times 10^{29} \int_o^P \chi_i dP \text{ in (meter)}^{-2}$$
$$= 2.12 \times 10^{25} \int_o^P \chi_i dP \text{ in (cm)}^{-2} \tag{1.41}$$

In the case of molecular oxygen, χ_i is taken as uniform and equal to 0.2096, giving

$$N_{O_2} = 0.4444 \times 10^{25} \text{ P cm}^{-2} \tag{1.42}$$

The lower boundary condition for ozone

The surface destruction process for ozone must give rise to a boundary layer effect in which the ozone changes rapidly from the free air value to a lower value at the ground. Our use of (approximately) 3-km height increments will not represent this adequately. Secondly, land and water surfaces differ markedly in their effect on surface ozone. Fortunately, it is possible to correct for both of these complications by using the detailed analysis by P. Fabian and C. Junge (Global rate of ozone destruction at the earth's surface: Arch. Meteor., Geo., Bioklimat., (a)-Meteor. u. Geo. 19, 161-72, 1970). The important point is to obtain the correct global ratio between the lower tropospheric value of ozone and the surface destruction rate, since the former may affect the ozone amount higher up and thereby the photochemical destruction rates.

Fabian and Junge model the presumed boundary-layer ozone profile by standard methods and make allowance for different properties of land, vegetation and water (and their global distribution) and for different wind speeds. They arrive at a global surface destruction rate ranging from 3.1 to 5.6×10^{10} mol/cm^2 sec., the variation being due to uncertainty in choice of surface wind speed. Using an average lower tropospheric value of 5×10^{11} mol/cm^3 for O_3, we have a global ratio of

$$d_1 \equiv \frac{3.1 \text{ to } 5.6 \times 10^{10}}{5 \times 10^{11}} \sim 0.08 \text{ cm sec}^{-1}$$

[Note that "measured" values of d at the ground range from .04 cm sec^{-1} over water to land values of 0.6 (Aldaz) and 1.0 (Galbally) cm sec^{-1}.]

Referring to our model equations (1.37) and (1.38)

$$\left(\frac{K_D}{H_0\Delta Z}\right)_{J-1/2}(\chi_{J-1}-\chi_J) = \frac{d\chi_{J-1}}{1+\left(\frac{dH_0\Delta Z}{K_D}\right)} = d\chi_J$$

we recognize the left side as the downward diffusive flux at the bottom of our model, (which must equal the surface destruction rate) and χ_{J-1} as the number density (mixing ratio) in the model corresponding most closely to the $5x10^{11}$ number density for the free air referred to above. Our model will not include different types of surface with their differing abilities to destroy ozone. This is alright since, because of the strong horizontal advection in the atmosphere, these differing surface properties affect primarily the local boundary layer profile and surface value rather than the local free troposphere values. We must use a correct global effect, however, and we get this by simply choosing a single model value for d such that the ratio of the destruction rate to the free air value in the model matches the global observed ratio, $\bar{d}$.

$$\frac{d}{1+\frac{dH_0\Delta Z}{K_D}} = d_1 = 0.08 \text{ cm/sec}$$

For $H_0\Delta Z$ = 3 Km, and K_d = 10 m^2 sec^{-1}, this gives d = 0.105 cm sec^{-1}. Fabian and Junge also discuss the ratio (their ε) of the surface value of O_3 to the free air value, and obtain typical values of 0.35 over land and 0.85 over water. Our model now implies a single value for this ratio of

$$\frac{\chi_J}{\chi_{J-1}} = \frac{d_1}{d} = 0.76$$

very comfortably located in the range inferred by Fabian and Junge.

Diffusivity for ozone

Vertical diffusivity

An upper estimate for K_d in the troposphere and lower stratosphere can be obtained from measured ozone profiles by equating

$$\left(\frac{48}{29}\right)\rho K_d \frac{\partial \chi}{\partial z} = \text{constant} = 3.5\text{x}10^{-12} \text{ gm/cm}^2\text{/sec}$$

where χ is the number density mixing ratio, and $3.5\text{x}10^{-12}$ is the product of the mass of an ozone molecule ($7.9\text{x}10^{-23}$gm) with the average global surface destruction rate of $4.4\text{x}10^{10}$ mol $\text{cm}^{-2}\text{sec}^{-1}$ found by Fabian and Junge (reference cited earlier). Values of $\partial\chi/\partial z$ can be obtained from the middle latitude synthesis by Krueger and Minzer (A proposed mid-latitude ozone model for the U.S. Standard Atmosphere. X-651-73-72, Goddard Space Flight Center). (Similar values are obtained from using the 3-year average ozone profiles for Bedford and Green Bay that has been analyzed by D. Wu). The results of this calculation are shown in Table 1.1.

At higher elevations ozone begins to no longer act as an inert tracer. Here we refer to computations by S. Wofsy and M. McElroy (On vertical mixing in the upper stratosphere and lower mesosphere. J. Geo. Res., 78, 2619-2624, 1973). These authors combine (a), the suggestion by Lindzen that K might vary as $\rho^{-1/2}$ because the velocities in gravity waves - a likely mixing process - tend to increase in this manner with height, and (b), measurements by Ehhalt of methane concentration. Using a chemical model, they find that Ehhalt's measurements at 50 km fit but with a K_d distribution having small values of $2\text{x}10^3$ cm^2 sec^{-1} at 16-20 km increasing to $2\text{x}10^6$ at 80 km as $(n_m)^{-1/2}$. We can model this simply by noting that n_m is proportional to p for constant T, and that p in turn is proportional to exp(-Z).

Table 1.1: Upper estimate for K_d in the troposphere and lower stratosphere

z(km)	$\left(\frac{48}{29}\chi\right)$	$\frac{48}{29}\frac{\partial\chi}{\partial z}(cm^{-1})$	$\rho\ \frac{gm}{cm^3}$	$K_d\ \frac{cm^2}{sec}$
2	5×10^{-8}			
3		0.5×10^{-13}	0.90×10^{-3}	7.80×10^{4}
4	6			
5		0.5	0.74	9.40×10^{4}
6	7			
7		1.5	0.59	4.00×10^{4}
8	10			
9		6	0.47	1.20×10^{4}
10	22			
11		15	0.36	0.65×10^{4}
12	52			
13		15	0.26	0.90×10^{4}
14	82			
15		30	0.19	0.61×10^{4}
16	142			
17		63	0.15	0.37×10^{4}
18	267			
19		82	0.11×10^{-3}	0.39×10^{4}
20	431×10^{-8}			

However, we believe that the three-dimensional model waves can sufficiently handle the vertical "diffusion" in the upper stratosphere and thus we have chosen the following distribution of K which essentially ignores vertical diffusion processes in the stratosphere.

(a) $Z \leq Z_0 = 0.6$: $K \equiv K_0 = 1 \times 10^5$ cm^2/sec

(b) $Z_0 < Z \leq Z_{10} = 2.4$: $K_1 = 1 \times 10^2$ cm^2/sec

$$K = K_0 + \frac{(K_1 - K_0)}{(Z_{10} - Z_0)} [(Z - Z_0) \cdot (2 \cdot Z_{10} - Z - Z_0)]^{1/2}$$

(c) $Z > Z_{10}$: $K = K_1$

The K_d values used in the model as obtained from the formulas are shown in Table 1.2 along with K_d values inferred from observed CH_4 (Wofsy and McElroy) and ozone profiles.

Table 1.2: Values of K_d from the model "formula" and inferred from O_3 and CH_4 profiles. K_d units are cm^2/sec.

z(km)	Z	Formula	Inferred (O_3)	Inferred (CH_4)
3	.357	100.0×10^3	78.0×10^3	300.0×10^3
5	.616	90.0	94.0	
7	.892	46.2	40.0	
9	1.171	26.5	12.0	
11	1.492	13.8	6.5	
13	1.802	6.3	9.0	
15	2.120	1.5	6.1	
17	2.433	0.1	3.7	2.0×10^3
19	2.719	0.1	3.9×10^3	
20	2.861	0.1		6.8
30	4.289	0.1		45.0
40	5.717	0.1		110.0
50	7.145	0.1		260.0
60	8.573	0.1		490.0
70	10.000	0.1×10^3		940.0×10^3

Horizontal diffusivity

The purpose of the horizontal diffusion term in our model is principally to account for the energy conversion of vertically propagating gravity waves into horizontal transportation in the upper mesospheric levels of the model atmosphere and to act as a "sponge" to prohibit wave refelctions from the fixed (i.e., vertical motion = 0) upper boundary. Thus, we have chosen to specify A_H as a function of Z/Z_{top} in the form

$$A_H = A_{const} \, (Z/Z_{top})^6 \; [m^2 s^{-1}] \qquad (1.21.3)$$

in which A_{const} is a specified constant. A value of $A_{const} = 6 \times 10^7 \; [m^2 s^{-1}]$ seems to work very well with the truncation specification of the current model version (18 wave) and has thus been adopted for all of its horizontal diffusion terms (i.e., for momentum, temperature and ozone diffusion).

Profiles for both the vertical diffusion coefficients K_d and for the horizontal diffusion coefficients A_H as represented at the model levels are shown in Table 2.2.

2. Choice of vertical levels.

We want the vertical domain to extend well above the actual ozone layer. We also want it high enough that there is some opportunity for the damping effects of ozone and radiation to absorb mechanical energy generated in the baroclinic processes of the lower atmosphere. On the other hand, we cannot for practical reasons get involved in the more complicated processes of the lower thermosphere. An upper limit of about 85 km seems reasonable.

We obtain equal intervals in $Z = -\ell nP$ (P = pressure ÷ 100 cb) by defining

$$\left.\begin{aligned} Z_j &= \Delta Z(J-j) \\ P_j &= e^{-\Delta Z(J-j)} \end{aligned}\right\} \quad j = 1, 2, \ldots, J. \tag{2.1}$$

j = 1 is at the "top" of our model atmosphere, and j = J at the bottom, whence

$$Z = \frac{Z_1}{J-1} = \frac{Z_{top}}{J-1}$$

A convenient choice is obtained by choosing

$$\begin{aligned} e^{\Delta Z} &= r, \quad r = 3/2 \\ \Delta Z &= \ell nr = 0.40547 \end{aligned} \tag{2.2}$$

so that

$$\begin{aligned} Z_1 &= Z_{top} = (J-1)\ell nr \\ P_1 &= r^{-(J-1)} \end{aligned} \tag{2.3}$$

Successive pressure levels are separated by (roughly) 85/31 ~ 2.7 km. The relations

$$P_j = r^{-(J-j)}; \; P_{j+1} = rP_j \tag{2.4}$$

are useful. At these levels, the following basic variables will be represented $j = 1, 2, \ldots, J$: T_j, W_j, $(\chi_i)_j$ together with the heating rate, the photochemical term, and the vertical turbulent fluxes of momentum. At the intermediate levels the streamfunction ψ_j will be represented

$$j = \frac{3}{2}, \frac{5}{2}, \ldots, J-\frac{1}{2} : \psi_j$$

For convenience in notation, however, ψ will be labeled with an interger subscript according to the convention

$$\psi(P = P_{j+1/2}) \equiv \psi_j \quad .$$

This results in the scheme as seen in Figure 2.1.

Table 2.1 lists the values of the more basic variables for the choice $r = 3/2$, $J = 32$. Values of $\overline{T}$ above 30 km were taken from the 1965 CIRA annual mean, values at lower elevation coming from data based on statistics gathered by the Planetary Circulation Project at M.I.T. (To be precise, they were obtained from the latter as shown in a figure based on them in the thesis by A. Hollingsworth). The static stability parameter S is defined later in equation (3.20). Table 2.2 contains the values for the vertical (K_m, K_d) and horizontal (A_H) diffusion coefficients (in units of m^2/s) at the same model levels as shown in Table 2.1. The basis for these values is discussed in the previous section.

Figure 2.1: Vertical levels of the model and the location on these levels of the model variables.

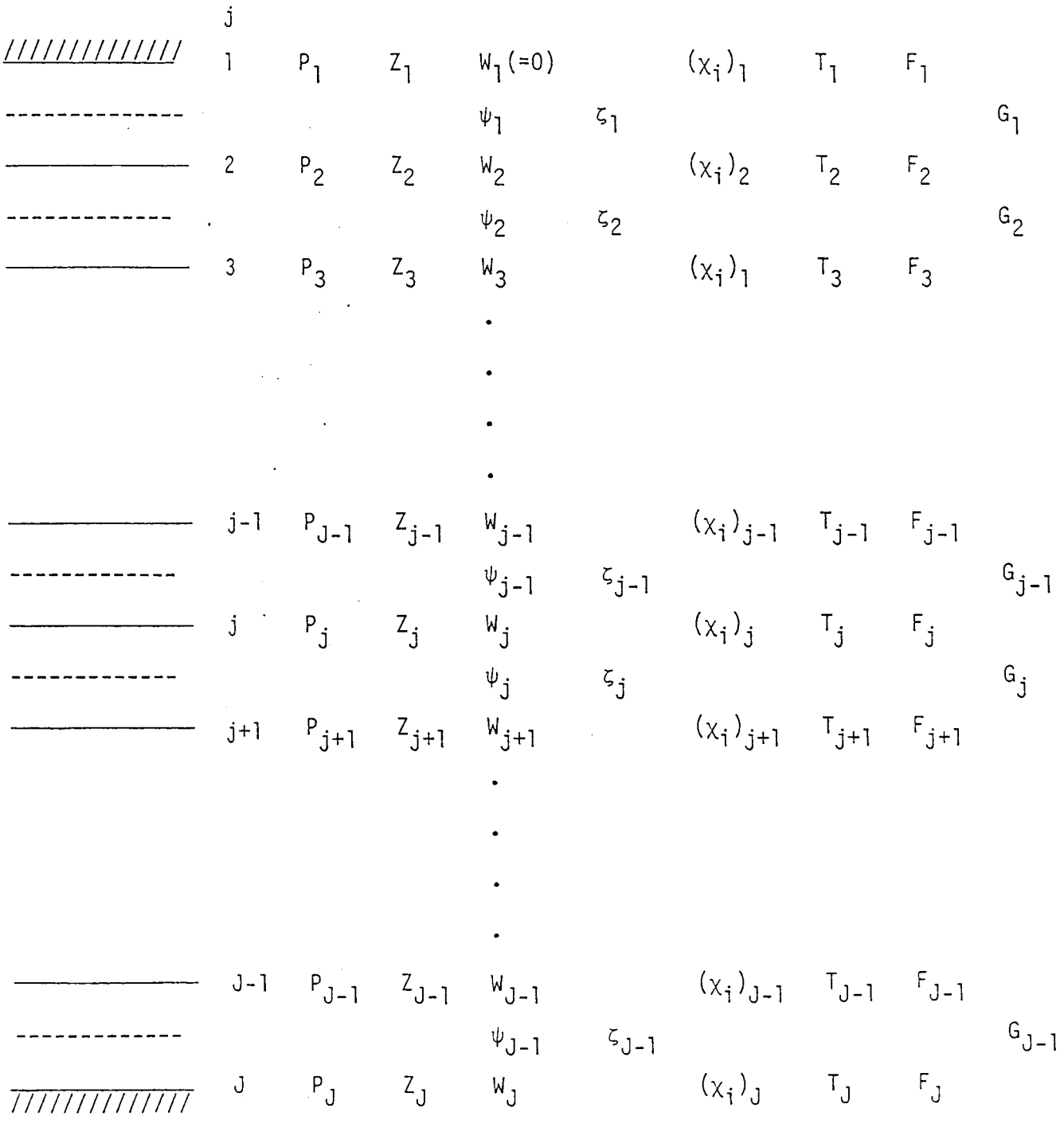

TABLE 2.1: Vertical layer designations and mean vertical profiles

j +	P_j	Z_j	z (km) (approx)	$\bar{T}_j$	n_m $(cm)^{-3}$	S_j
1	.00000348	12.569	85.4	181.0	139×10^{12}	173
2	.00000522	12.164	83.2	181.0	209	173
3	.00000782	11.758	81.0	181.0	313	162
4	.0000117	11.353	78.8	183.5	463	130
5	.0000176	10.948	76.5	192.0	664	111
6	.0000264	10.542	74.1	201.0	952×10^{12}	114
7	.0000396	10.137	71.6	211.0	136×10^{13}	137×10^{-4}
8	.0000594	9.731	69.0	219.0	196	144
9	.0000891	9.326	66.3	226.5	285	154
10	.000134	8.920	63.5	234.0	415	161
11	.000200	8.515	60.6	241.5	600	166
12	.000301	8.109	57.6	249.6	877×10^{13}	167
13	.000451	7.704	54.5	258.5	126×10^{14}	174
14	.000677	7.298	51.4	267.0	184	217
15	.00101	6.893	48.2	267.5	274	277
16	.00152	6.488	45.0	261.5	421	302
17	.00228	6.082	41.9	254.5	649×10^{14}	295
18	.00343	5.677	38.8	248.5	100×10^{15}	285
19	.00514	5.271	35.9	242.5	154	277
20	.00771	4.866	33.0	237.0	236	272
21	.0116	4.460	30.2	231.0	364	269
22	.0173	4.055	27.5	225.0	557	261
23	.0260	3.649	24.8	219.5	855×10^{15}	251
24	.0390	3.244	22.2	214.5	132×10^{16}	237
25	.0585	2.838	19.6	211.5	201	217
26	.0878	2.433	17.1	210.5	302	194
27	.132	2.027	14.6	213.0	499	155
28	.198	1.622	12.0	222.0	646	125
29	.296	1.216	9.3	234.0	913×10^{16}	116
30	.444	0.811	6.4	253.0	130×10^{17}	104
31	.667	0.405	3.4	272.0	182	105
32	1.000	0.0	0.1	287.0	265×10^{17}	122

TABLE 2.2: Profiles for the vertical and horizontal diffusion coefficients

j	Z_j	K_m, K_D (m^2/s)	A_H (m^2/s)
1	12.569	9.997×10^{0}	6.000×10^{7}
2	12.164	8.044	4.928
3	11.758	6.449	4.021
4	11.353	5.147	3.258
5	10.948	4.083	2.619
6	10.542	3.201	2.088
7	10.137	2.506	1.650
8	9.731	1.928	1.292
9	9.326	1.455	1.001
10	8.920	1.069	7.665×10^{6}
11	8.515	7.544×10^{-1}	5.798
12	8.109	4.972	4.327
13	7.704	2.872	3.108
14	7.298	1.157	2.299
15	6.893	1.000×10^{-2}	1.632
16	6.488	1.000	1.134
17	6.082	1.000	7.701×10^{5}
18	5.677	1.000	5.090
19	5.271	1.000	3.263
20	4.866	1.000	2.019
21	4.460	1.000	1.198
22	4.055	1.000	6.760×10^{4}
23	3.649	1.000	3.593
24	3.244	1.000	1.772
25	2.838	1.000	7.954×10^{3}
26	2.433	1.000×10^{-2}	3.154
27	2.027	2.265×10^{-1}	1.056
28	1.622	9.917×10^{-1}	2.769×10^{2}
29	1.216	2.473	4.928×10^{1}
30	0.811	5.308	4.327
31	0.405	10.000	6.760×10^{-2}

3. Non-dimensional finite-difference equations

In this section we write the basic equations in a non-dimensional form (primarily to simplify the dynamical computations) and simultaneously introduce the vertical finite-difference representation defined in Section 2. We define

$$
\begin{aligned}
\mu &= \sin\phi \\
\nabla(\text{dim}) &= \frac{1}{a}\,\nabla(\text{non-dim}) \\
\nabla^2(\text{dim}) &= \frac{1}{a^2}\,\nabla^2(\text{non-dim}) \\
\psi(\text{dim}) &= 2\Omega a^2\,\psi(\text{non-dim}) \\
X(\text{dim}) &= 2\Omega a^2\,X(\text{non-dim}) \\
t(\text{dim}) &= \frac{1}{2\Omega}\,t(\text{non-dim}) \\
W(\text{dim}) &= 2\Omega\,W(\text{non-dim}) \\
A_H(\text{dim}) &= 2\Omega a^2\,A_H(\text{non-dim}) \\
T(\text{dim}) &= (4\Omega^2a^2/R)\,\overline{T}(\text{non-dim}) + (4\Omega^2a^2/R)\,T(\text{non-dim})
\end{aligned}
\qquad (3.1)
$$

In the last expression T (dim) is the "total" temperature in absolute degrees, $\overline{T} = \overline{T}(Z)$ is the "standard atmosphere" temperature (also in degrees) given in the table at the end of Section 2, while the quantity $(4\Omega^2a^2/R)\,T$ (non-dim) is the (deviation from the horizontal mean) variable T appearing in (1.25), having a zero horizontal average. [The total T (dim) is, of course, used in all chemical computations].

$$
\begin{aligned}
\Omega &= 2\pi/8.64\times10^4 \text{ rad sec}^{-1} \\
a &= 6.371\times10^6 \text{ meters} \\
R &= 287 \text{ kJ ton}^{-1} \text{ deg}^{-1} \\
Cp &= (7/2)R
\end{aligned}
\qquad (3.2)
$$

One day, $(2\pi/\Omega)$ secs, corresponds to

$$\Delta t(\text{non-dim}) = 2\Omega(\frac{2\pi}{\Omega}) = 4\pi \quad . \tag{3.3}$$

The non-dimensional ∇^2 operator is

$$\nabla^2(\ ) = \frac{1}{\cos^2\phi}\frac{\partial^2(\ )}{\partial\lambda^2} + \frac{1}{\cos\phi}\frac{\partial}{\partial\phi}\left[\cos\phi\frac{\partial(\ )}{\partial\phi}\right] \quad . \tag{3.4}$$

The relation

$$PW = \nabla^2 X \tag{1.16}$$

between W and X can be used to eliminate X in favor of W [in equation (1.13)] by defining the inverse Laplacian operator

$$\left.\begin{aligned} L &\equiv \nabla^{-2} \\ X &= PLW \end{aligned}\right\} \tag{3.5}$$

We also have

$$\zeta = \nabla^2\psi \ ; \ \psi = L\zeta \tag{3.6}$$

A further convenient arrangement is useful for evaluating terms of the form $\partial(PF)/\partial P$, which appears in the vertical diffusion terms for vorticity and trace substances and in the term

$$\frac{\partial X}{\partial P} = \frac{\partial}{\partial P}[P(LW)]$$

in the vorticity equation (1.13). We have

$$\left[\frac{\partial}{\partial P}(PF)\right]_j = \frac{P_{j+1/2}\,F_{j+1/2} - P_{j-1/2}\,F_{j-1/2}}{P_{j+1/2} - P_{j-1/2}} = \left(\frac{r}{r-1}\right)F_{j+1/2} - \left(\frac{1}{r-1}\right)F_{j-1/2} \tag{3.7}$$

where we have made use of (2.4).

The horizontal advection of a quantity F can be written as the Jacobian

$$-\vec{v}_\psi \cdot \nabla F = -\hat{k}x\nabla\psi \cdot \nabla F = \frac{\partial F}{\partial \lambda}\frac{\partial \psi}{\partial \mu} - \frac{\partial \psi}{\partial \lambda}\frac{\partial F}{\partial \mu}$$

$$\equiv J(F,\psi) \tag{3.8}$$

The non-dimensional form of the vorticity equation (1.13), with regard to the subscript labelling defined in Section 2, together with equation (1.21) and (3.5) - (3.8) is as follows:

For $j = 1, 2, \ldots, J-1$:

$$\frac{\partial \zeta_j}{\partial t} = J(\mu+\zeta_j,\psi_j) - \nabla\cdot\{\mu\nabla L[(\frac{r}{r-1})W_{j+1} - (\frac{1}{r-1})W_j] +$$

$$+ (\frac{r}{r-1})F_{j+1} - (\frac{1}{r-1})F_j + A_H)_j[\nabla^4\psi_j + 2\nabla^2\psi_j] \tag{3.9}$$

$$\psi_j = L\zeta_j \tag{3.10}$$

$$F_1 = 0 \tag{3.11}$$

$$F_J = -D\zeta_{J-1} \tag{3.12}$$

$$F_j = E_j(\zeta_j - \zeta_{j-1}) \qquad (j = 2, 3, \ldots, J-1) \tag{3.13}$$

$$E_j = (K_m)_j \div [H_0^2 2\Omega\Delta Z] \tag{3.14}$$

$$D = k_D \div 2\Omega \tag{3.15}$$

$$W_1 = 0 \tag{3.16}$$

$$W_J = -J(\frac{h}{H_0}, \psi_{J-1}) \tag{3.17}$$

The non-dimensional form of the "thermal wind equation" (1.9) becomes for

$j = 2, 3, \ldots, J-1$:

$$\nabla\cdot\mu\nabla(\psi_j-\psi_{j-1}) = -\nabla^2 T_j \Delta Z \tag{3.18}$$

The non-dimensional form of the thermal equation (1.25) becomes for

$j = 2, 3, \ldots, J-1$:

$$\frac{\partial T_j}{\partial t} = \frac{1}{2} J(T_j, \psi_j+\psi_{j-1}) - S_j W_j + A_H)_j \nabla^2 T_j + \left[\frac{R}{C_p 8\Omega^3 a^2}\right] \tag{3.19}$$

where

$$S_j = \left(\frac{R}{4\Omega^2 a^2}\right) \left[\frac{d\overline{T}}{dZ} + \frac{R}{C_p}\overline{T}\right]_j \tag{3.20}$$

is tabulated at the end of Section 2. Note that q_j, the rate of heating per unit mass, is still in dimensional form in (3.19). It is considered later in Section F.

The trace substance is, for

$j = j_o, j_o+1, \ldots, J-1$:

$$\frac{\partial \chi_j}{\partial t} = \frac{1}{2} J(\chi_j, \psi_j+\psi_{j-1}) - W_j\left(\frac{d\overline{\chi}}{dZ}\right) + \left(\frac{r}{r-1}\right)G_j - \left(\frac{1}{r-1}\right)G_{j-1} + A_H)_j \nabla^2 \chi_j +$$

$$+ \left(\frac{1}{2\Omega}\right)\left[\frac{1}{n_m}\left(\frac{dn}{dt}\right)_c\right]_j \tag{3.21}$$

$$\left.\begin{aligned} G_j &= D_j(\chi_{j+1}-\chi_j) \ ; \quad \text{for } j=j_o, \ldots, J-2 \\ D_j &= (K_d)_{j+1/2} \div (2\Omega H_0^2 \Delta Z) \end{aligned}\right\} \tag{3.22}$$

[The vertical diffusion coefficient K_d is defined at the Z_j-levels corresponding

to j = integer plus 1/2, whereas the vertical exchange coefficient K_m for vorticity, appearing in (3.14), is defined at interger values of j.] At the bottom, the relation (1.38) gives

$$G_{J-1} = - \frac{X_{J-1}}{\left[\frac{2\Omega H_0}{d} + \frac{2\Omega H_0^2 \Delta Z}{(K_d)_{J-1/2}}\right]} \tag{3.23}$$

The integer j_o sets the level above which (3.21) may be replaced by a photochemical equilibrium statement, as discussed near the end of Section 1.

4. Model chemistry

The distribution of ozone in the model is determined by the following chemical reactions (with rate constants given by Baulch et al., 1982)

1.	$NO + O_3 \rightarrow NO_2 + O_2$	$k_3 = 3.6 \times 10^{-12} e^{-\frac{1560}{T}}$
2.	$NO_2 + O \rightarrow NO + O_2$	$k_4 = 9.3 \times 10^{-12}$
3.	$NO_2 + h\nu \rightarrow NO + O$	J_{NO_2}
4.	$OH + O_3 \rightarrow HO_2 + O_2$	$k_{12} = 1.9 \times 10^{-12} e^{-\frac{1000}{T}}$
5.	$OH + O \rightarrow H + O_2$	$k_{14} = 2.3 \times 10^{-11} e^{\frac{110}{T}}$
6.	$H + O_2 + M \rightarrow HO_2 + M$	$k_{16} = 5.9 \times 10^{-32} \left(\frac{T}{300}\right)$
7.	$H + O_3 \rightarrow OH + O_2$	$k_{17} = 1.4 \times 10^{-10} e^{-\frac{480}{T}}$
8.	$HO_2 + O \rightarrow OH + O_2$	$k_{18} = 3.7 \times 10^{-11}$
9.	$HO_2 + O_3 \rightarrow OH + 2O_2$	$k_{20} = 1.4 \times 10^{-14} e^{-\frac{600}{T}}$
10.	$O_3 + O \rightarrow 2O_2$	$k_{22} = 1.8 \times 10^{-11} e^{-\frac{2300}{T}}$

11. $O_3 + h\nu \rightarrow O + O_2$ $\qquad J_{O_3}$

12. $O + O_2 + M \rightarrow O_3 + M$ $\qquad \ell_{25} = 6.2 \times 10^{-34} \left(\frac{T}{300}\right)^{-2.0}$

13. $O_2 + h\nu \rightarrow 2O$ $\qquad J_{O_2}$

14. $ClO + O \rightarrow Cl + O_2$ $\qquad k_{31} = 7.5 \times 10^{-11} e^{-\frac{120}{T}}$

15. $ClO + NO \rightarrow Cl + NO_2$ $\qquad k_{32} = 6.2 \times 10^{-12} e^{\frac{294}{T}}$

18. $O + O + M \rightarrow O_2 + M$ $\qquad \ell_{37} = 4.8 \times 10^{-38} e^{\frac{900}{T}}$

19. $NO + HO_2 \rightarrow NO_2 + OH$ $\qquad k_{38} = 3.7 \times 10^{12} e^{\frac{240}{T}}$

We assume chemical equilibrium determines the NO/NO_2 balance, the Cl/ClO balance, and the $OH/OH_2/H$ balance. Thus, we assume

$$k_3[NO][O_3] + k_{32}[ClO][NO] + k_{38}[NO][HO_2] = k_4[NO_2][O] + [NO_2]J_{NO_2} \qquad (4.1)$$

$$k_{14}[OH][O] = k_{16}[H][O_2][M] + k_{17}[H][O_3] \qquad (4.2)$$

$$k_{17}[H][O_3] + k_{18}[HO_2][O] + k_{38}[NO][HO_2] + k_{20}[HO_2][O_3] = k_{12}[OH][O_3] + k_{14}[OH][O]. \qquad (4.3)$$

We also assume that the O/O_3 balance is determined by the principal terms only:

$$[O_3]J_{O_3} = \ell_{25}[O][O_2][M] \qquad (4.4)$$

With these assumptions the chemical loss of odd oxygen is given by

$$[M]\left(\frac{\partial \chi_{O_x}}{\partial t}\right)_c = 2[O_2]J_{O_2} - 2k_4[NO_2][O] - 2k_{12}[OH][O_3] - 2k_{12}[OH][O_3]$$
$$- 2k_{14}[OH][O] - 2k_{22}[O_3][O] - 2k_{31}[ClO][O] \qquad (4.5)$$
$$- 2\ell_{37}[O]^2[M] + 2k_{38}[NO][HO_2].$$

Two-dimensional daily-averaged solsticial distributions of the mixing ratios of NO_x, ClO, and OH have been provided by Dak Sze (see Figures 1-3). We have assumed that these distributions are appropriate for January 1 and that the distributions evolve sinusoidally in an annual wave throughout the year. Most of the chemistry in the model is active only during the hours of sunlight. Therefore, we solve the above chemical equilibrium equations for the average species concentrations during daylight hours. The equations result in a quadratic equation for [NO]. The solution to this equation then readily provides daytime values of $[NO_2]$ and $[HO_2]$. These daytime values are then inserted into equation (4.5) and the entire right hand side of the equation is multiplied by h_s/π (see Section 5).

There exist conditions for which the above determination of the chemical loss of odd oxygen may be inappropriate. Note, in particular, that we are assuming the complete absence of chemistry in the polar night. We have ignored the photodissociation of NO which occurs above 50 km; this means that the calculated NO/NO_2 ratio will be incorrect at high altitudes, but this should not affect the other ratios we calculate.

The numerical model uses half-hour time steps (Δt). Stability of the model then requires a way to predict O_x when its chemical time constant is less than or equal to approximately 0.5 hours. The following procedure is used:

At the start of each N-cycle we calculate $0.42[\bar{J}_{O_2}]$ where $[\bar{J}_{O_2}]$ is the zonal-mean daily-average photodissociation rate of molecular oxygen at each of the Gaussian latitudes. We also calculate

$$TC = [\chi_{O_x}] - 0.42[\bar{J}_{O_2}] \cdot (0.7 \times \pi \times \Delta t). \tag{4.6}$$

At those latitudes and levels where $TC > 0$, a chemical equilibrium value of O_x is calculated by setting the RHS of equation (4.5) equal to zero and with the O/O_3 ratio being determined by equation (4.4). At these locations $(\partial \chi_{O_x}/\partial t)_c$ is simultaneously set equal to zero. A prediction is then made on χ_{O_x} in the spectral domain. Next, χ_{O_x} is transformed back to the grid domain and at the locations where chemical equilibrium applies, the predicted value of χ_{O_x} is then partitioned into ozone and atomic oxygen according to equation (4.4). Finally, χ_{O_x} and χ_{O_3} are transformed back into the spectral domain.

The effect of the above procedure on the odd oxygen budget has been analyzed in Cunnold (1983) for the 6 wave model. In that report it was noted that the boundary between the regions where photochemical equilibrium is assumed and where it is not, constitutes a discontinuity which, because of the spectral representation of model variables, produces minor numerical effects on the ozone budget at all latitudes. We found, furthermore, that these effects are minimized if the chemical computation starts from the χ_{O_x} grid field and not from χ_{O_3} field. This is because, at high altitudes, strong gradients of χ_{O_3} (but not of χ_{O_x}) exist across the polar night boundary which are poorly represented by the spectral model.

In treating the chemistry we use p/kT for the concentration of air molecules in the atmosphere and 0.21 times this value for the concentration of oxygen mole-

cules. To increase the efficiency of the computation of reaction rates which are calculated at every time step, we approximate each rate constant as a product of the variables exp(-125/T) and exp(-300/T).

References

Baulch, D.L., R.A. Cox, P.J. Crutzen, R.F. Hampson, Jr., J.A. Kerr, J. Troe, and R.T. Watson, Evaluated kinetic and photochemical data for atmospheric chemistry: Supplement 1. CODATA task group on chemical kinetics, J. Phys. Chem. Ref. Data, 11, 327-496, 1982.

Cunnold, D.M., 1983: The impact of the photochemical equilibrium assumption in a dynamical-chemical model on the calculated distribution of odd oxygen in the upper stratosphere and mesosphere. Georgia Institute of Technology Internal Report, January 1983.

5. The calculation of photodissociation rates and the associated heating

Photodissociation rates and heating rates due to the absorption of solar radiation by molecular oxygen, ozone, and nitrogen dioxide are evaluated in the model.

The vertically overhead column of ozone is first evaluated through the integration

$$N_{O_3}(P_j) = 2.1156 \times 10^{25} \int_0^{P_j} \chi_{O_3} \, dP \ cm^{-2} . \tag{5.1}$$

We assume that χ_{O_3} varies linearly with Z in the interval j to j+1. Then

$$N_{O_3}(P_J) = 2.1156 \times 10^{25} \left\{ \sum_{j=2}^{J} \left(1 - \frac{r-1}{r\Delta Z}\right) P_j \chi_j + \sum_{j=1}^{J-1} \left(\frac{r-1}{\Delta Z} - 1\right) P_j \chi_j \right\} \tag{5.2}$$

To increase computational efficiency the longitudinal variation of the photodissociation rates is approximated using the following procedure. At each time step the mean and standard deviation of the column ozone is obtained at each latitude and level. The photodissociation and heating rates are then evaluated for the two ozone columns equal to the mean ±1 standard deviation. For example, the photodissociation rate of ozone is

$$J_{O_3} = \Sigma \, \alpha_{O_3}(\lambda_i) F(\lambda_i) e^{-\left\{\alpha_{O_3}(\lambda_i)\chi_{O_3} + \alpha_{O_2}(\lambda_i)\chi_{O_2}\right\}} \ sec^{-1} \tag{5.3}$$

where the absorption coefficients of molecular oxygen (α_{O_2}) and ozone (α_{O_3}) and the integrated photon flux in each wavelength interval ($F(\lambda_i)$) are given in

Table 5.1. The tabulated values of F have been taken from page B-10 of "The Stratosphere, 1981." The ozone absorption coefficients are from Inn and Tanaka but adjusted by the Vigroux temperature correction factors for -44°C as recommended by Klenk (1981). At visible wavelengths, the values are from Ackermann (1971). The absorption coefficients of NO_2 are from Table A-5 of "The Stratosphere, 1981." The absorption cross sections of O_2 in the Hartley continuum is from Table 1-33 of "The Stratosphere: Present and Future, 1979." In the Schumann-Runge bands we use the mean of the high and low values given by Kockarts (1971), a choice which is consistent with the recent work of Frederick and Hudson (1980). To account for the backscattering of energy from the lower atmosphere, we increase all of the solar fluxes at wavelengths greater than 3125Å by a factor of 1.5.

Heating rates are computed in a similar manner. The heating rate, due to the absorption of ultraviolet and visible radiation by ozone is given by

$$\frac{q}{C_P} = 9.453 \times 10^7 \chi_{O_3} \sum_i \alpha_{O_3}(\lambda_i) F(\lambda_i) \frac{1}{\lambda_i} e^{-\left\{\alpha_{O_3}(\lambda_i) X_{O_3} + \alpha_{O_2}(\lambda_i) X_{O_2}\right\}}. \quad (5.4)$$

This is in dimensionless units and is a term in equation (1.25). Here χ_{O_3} is the ozone volume mixing ratio.

In equations (5.3) and (5.4), X_{O_3} and X_{O_2} are the column densities of ozone and molecular oxygen. (For typical globally-averaged values, see Table 5.2).

$$X_{O_3} = N_{O_3}(P_J) \sec \psi \ cm^{-2}$$

$$X_{O_2} = 2.1156 \times 10^{25} P_J \sec \psi \ cm^{-2}$$

TABLE 5.1: Flux of solar photons, q, at one AU, absorption cross section of O_2 and of O_3, $\sigma(O_2)$ and $\sigma(O_3)$, for wavelength intervals $\Delta\lambda$ and wavenumber intervals $\Delta\nu$.

No.	$\Delta\lambda$(Å)	$\Delta\nu(cm^{-1})$	$q(cm^{-2}s^{-1})$	$\sigma(O_2)(cm^2)$	$\sigma(O_3)(cm^2)$	$\sigma(NO_2)(cm^2)$
45	1.754-1.739	57.000-57.500	1.33×10^{11}	2.74×10^{-19}		
46	1.770-1.754	56.500-57.000	1.61	1.40×10^{-20}		
47	1.786-1.770	56.000-56.500	2.00	9.00×10^{-21}		
48	1.802-1.786	55.500-56.000	2.20	5.00		
49	1.818-1.802	55.000-55.500	3.18	3.20		
50	1.835-1.818	54.500-55.000	3.30	2.00		
51	1.852-1.835	54.000-54.500	3.14	1.20		
52	1.869-1.852	53.500-54.000	3.71	5.00×10^{-22}		
53	1.887-1.869	53.000-53.500	4.96	3.00	5.70×10^{-19}	
54	1.905-1.887	52.500-53.000	5.57	1.30	5.15	
55	1.923-1.905	52.000-52.500	6.34	7.00×10^{-23}	4.66	
56	1.942-1.923	51.500-52.000	6.53	4.50	4.25	
57	1.961-1.942	51.000-51.500	9.01	2.90	3.99	
58	1.980-1.961	50.500-51.000	1.02×10^{12}	2.10	3.58	
59	2.000-1.980	50.000-50.500	1.15	1.70	3.20	
60	2.020-2.000	49.500-50.000	1.40	1.50	3.09	
61	2.041-2.020	49.000-49.500	1.69	1.25	3.09	3.25×10^{-19}
62	2.062-2.041	48.500-49.000	2.07	1.00	3.35	3.75
63	2.083-2.062	48.000-48.500	2.52	9.80×10^{-24}	4.04	3.79
64	2.105-2.083	47.500-48.000	4.21	9.20	4.91	3.85
65	2.128-2.105	47.000-47.500	7.23	8.50	6.37	3.92
66	2.150-2.128	46.500-47.000	7.79	7.85	8.32	3.98
67	2.174-2.150	46.000-46.500	8.45	7.05	1.09×10^{-18}	4.01
68	2.198-2.174	45.500-46.000	1.05×10^{13}	6.15	1.46	3.98
69	2.222-2.198	45.000-45.500	1.19	5.50	1.88	3.81
70	2.247-2.222	44.500-45.000	1.51	4.75	2.41	3.46
71	2.273-2.247	44.000-44.500	1.33	4.05	3.08	3.08
72	2.299-2.273	43.500-44.000	1.31	3.35	3.86	2.67
73	2.326-2.299	43.000-43.500	1.51	2.70	4.71	2.33
74	2.353-2.326	42.500-43.000	1.32	2.20	5.62	1.68
75	2.381-2.353	42.000-42.500	1.50	1.65	6.72	1.21
76	2.410-2.381	41.500-42.000	1.34	1.20	7.62	7.50×10^{-20}
77	2.439-2.410	41.000-41.500	2.02	7.50×10^{-25}	8.66	5.22
78	2.469-2.439	40.500-41.000	1.82		9.74	4.20
79	2.500-2.469	40.000-40.500	1.88		1.04×10^{-17}	3.30
80	2.532-2.500	39.500-40.000	1.83		1.09	2.36
81	2.564-2.532	39.000-39.500	2.25		1.10	1.45
82	2.597-2.564	38.500-39.000	4.65		1.07	1.72
83	2.632-2.597	38.000-38.500	4.44		1.02	1.95
84	2.667-2.632	37.500-38.000	1.07×10^{14}		9.40×10^{-18}	2.05
85	2.703-2.667	37.000-37.500	1.18		8.24	2.80

Table 5.1 Continued

No.	$\Delta\lambda$(Å)	$\Delta\nu$(cm^{-1})	q($cm^{-2}s^{-1}$)	$\sigma(O_2)(cm^2)$	$\sigma(O_3)(cm^2)$	$\sigma(NO_2)(cm^2)$
86	2.740-2.703	36.500-37.000	1.08×10^{14}		6.69×10^{-18}	3.50×10^{-20}
87	2.778-2.740	36.000-36.500	1.04		5.13	4.32
88	2.817-2.778	35.500-36.000	7.54×10^{13}		3.75	5.60
89	2.857-2.817	35.000-35.500	1.48×10^{14}		3.09	6.30
90	2.899-2.857	34.500-35.000	2.17		1.62	6.77
91	2.941-2.899	34.000-34.500	3.46		1.00	7.50
92	2.985-2.941	33.500-34.000	3.39		5.81×10^{-19}	9.10
93	3.030-2.985	33.000-33.500	3.24		3.85	1.17×10^{-19}
94	3.077-3.030	32.500-33.000	4.40		1.66	1.70
95	3.100(±25)	32.520-32.000	4.95		9.37×10^{-20}	1.83
96	3.150	32.000-31.496	5.83		4.52	2.19
97	3.200	31.496-31.008	6.22		2.53	2.35
98	3.250	31.008-30.534	6.96		1.19	2.54
99	3.300	30.534-30.075	8.61		5.54×10^{-21}	2.91
100	3.350	30.075-29.630	8.15		2.73	3.14
101	3.400	29.630-29.197	8.94		1.38	3.23
102	3.450	29.197-28.777	8.44		8.39×10^{-22}	3.43
103	3.725±250	28.777-25.127	9.85		4.30×10^{-23}	4.95
104	4.225	25.127-22.346	1.88×10^{16}		5.95	*5.30
105	4.725	22.346-20.100	2.40		5.29×10^{-22}	*3.30
106	5.225	20.100-18.265	2.46		2.11×10^{-21}	*2.00
107	5.725	18.265-16.736	2.61		4.21	$*7.00\times10^{-20}$
108	6.225	16.736-15.444	2.63		3.80	
109	6.900±425	15.444-13.605	4.32		1.28	

* Photodissociation of NO_2 is assumed to occur for $\lambda < 3975$Å.

TABLE 5.2: Typical concentrations of ozone, molecular oxygen, and nitrogen dioxide.

Level	Height km	$n(O_2)$ (cm^{-3})	Column Conc. $N_{O_2}(cm^{-2})$	$n(O_3)$ cm^{-3}	Column Conc. $N^*_{O_3}(cm^{-2})$	$n(NO_2)$ cm^{-3}
1	71.6	2.86×10^{14}	1.76×10^{20}	2.8×10^{8}	8.12×10^{13}	
2	69.0	4.11	2.64	6.4	1.97×10^{14}	
3	66.3	5.99	3.96	1.5×10^{9}	4.70	
4	63.5	8.72	5.94	3.5	1.13×10^{15}	
5	60.6	1.26×10^{15}	8.91	6.5	2.52	
6	57.6	1.84	1.34×10^{21}	1.2×10^{10}	5.16	
7	54.5	2.65	2.01	2.3	1.03×10^{16}	
8	51.4	3.86	3.01	4.6	2.08	
9	48.2	5.75	4.51	9.9	4.30	
10	45.0	8.84	6.77	2.15×10^{11}	9.01	8.84×10^{6}
11	41.9	1.36×10^{16}	1.02×10^{22}	4.1	1.84×10^{17}	7.79×10^{7}
12	38.8	2.10	1.52	7.6	3.55	4.00×10^{8}
13	35.9	3.23	2.28	1.3×10^{12}	6.50	1.39×10^{9}
14	33.0	4.96	3.43	1.8	1.09×10^{18}	2.60
15	30.2	7.64	5.14	2.45	1.68	3.27
16	27.5	1.17×10^{17}	7.71	3.4	2.46	3.40
17	24.8	1.80	1.16×10^{23}	4.3	3.48	3.68
18	22.2	2.84	1.73	4.8	4.66	3.96
19	19.6	4.22	2.60	4.65	5.87	4.40
20	17.1	6.34	3.90	3.6	6.92	6.04
21	14.6	9.43	5.85	2.5	7.68	8.08
22	12.0	1.34×10^{18}	8.78	2.0	8.25	1.15×10^{10}
23	9.3	1.92	1.32×10^{24}	1.0	8.66	1.72
24	6.4	2.73	1.98	6.0×10^{11}	8.88	2.58
25	3.4	3.82	2.96	6.0	9.05	3.87
26	0.1	5.56	4.44	6.0	9.25	5.80

ψ is the solar zenith angle which is determined from

$$\cos \psi = \sin\phi \sin\delta + \cos\phi \cos\delta \cos h \qquad (5.5)$$

where ϕ is latitude, δ is the solar declination and h is the hour angle (measured from local noon).

An additional approximation is used in deriving photodissociation and heating rates. The equations require average photodissociation rates during daylight hours and heating rates averaged over a 24-hour period. This averaging is accomplished by evaluating the rates at two preselected hour angles. If h_s is the hour angle of sunset, it is given by

$$\cos h_s = - \tan\phi \tan\delta.$$

Considering only the Northern Hemisphere ($\tan \phi \geq 0$), we have

$$\tan\phi \tan\delta \leq -1 : \quad h_s \equiv 0 \text{ (polar night)}$$

$$-1 \leq \tan\phi \tan\delta \leq 0 : \quad 0 \leq h_s \leq \frac{\pi}{2}$$

$$0 \leq \tan\phi \tan\delta \leq 1 : \quad \frac{\pi}{2} \leq h_s \leq \pi$$

$$1 \leq \tan\phi \tan\delta : \quad h_s = \pi \text{ (polar day)}$$

The daylight-average photodissociation and heating rates are determined as the average of the values at $h = h_s/4$ and $3h_s/4$. Empirically, we have found that by dividing the result by 1.025 we remove a slight bias in the results. Our studies indicate, moreover, that the approximation is accurate to better than 5% (see also, Cogley and Borucki, 1976). Twenty-four hour averages are determined by multiplying by h_s/π.

Using the above procedure, the photodissociation and heating rates are determined at each latitude and level for ozone columns equal to the zonal mean ([X]) ± 1 longitudinal standard deviation (σ). Suppose the results are J_+ and J_-. The photodissociation and heating rates produced by ozone and molecular oxygen are calculated at each longitude from

$$J = (J_+ J_-)^{1/2} \left(\frac{J_+}{J_-}\right)^{\frac{X-[X]}{2\sigma}} . \qquad (5.6)$$

NO_2 heating and dissociation rates are considered to depend little on the O_3 column. For these terms $(J_+ J_-)^{1/2}$ is used at all longitudes.

References

Ackerman, M., 1971: Ultraviolet solar radiation related to mesospheric processes. In Mesospheric models and related experiments, ed. G. Fiocco, D. Reidel Publishing Co., Dordrecht, Holland, pp. 149-159.

Cogley, A.C., and W.J. Borucki, 1976: Exponential approximation for daily average solar heating or photolysis, J. Atmos. Sci., 33, 1347-1356.

Frederick, J.E., and R.D. Hudson, 1980: Dissociation of molecular oxygen in the Schumann-Runge bands, J. Atmos. Sci., 37, 1099-1106.

Inn, E.C.Y., and T. Tanaka, 1953: Absorption coefficients of ozone in the ultraviolet and visible regions, J. Opt. Soc. Amer., 113, 870-873.

Klenk, K.F., 1980: Absorption coefficients of ozone for the backscattered UV experiment, Appl. Optics, 19, 236-242.

Kockarts, G., 1971: Penetration of solar radiation in the Schumann-Runge bands of molecular oxygen. In Mesospheric models and related experiments, ed. G. Fiocco, pp. 160-176, D. Reidel Publ. Co., Dordrecht, Holland.

Vigroux, E., 1953: Contributions a' l'etude experimentale de l'absorption de l'ozone, Am. Phys., 8, 709-762.

6. Tropospheric and infra-red stratospheric heating rates

In the troposphere and lower stratosphere, we follow Trenberth (Ph.D. thesis, M.I.T., 1972) in setting, at each level j,

$$\frac{\partial T}{\partial t} = \text{---} + h_j(T_j^* - T) \tag{6.1}$$

where h_j is a "Newtonian" cooling coefficient, T_j^* is a hypothetical equilibrium temperature field, and T is the temperature predicted by the model. (All T's in the above equation have a zero horizontal average.) For the zonally symmetric part, Trenberth divided T^* into an annual average term (symmetric in latitude) and a seasonal term (an odd function of latitude):

$$T_j^*(\mu,t) = T_{j2}^* P_2^0(\mu) + [T_{j1}^* P_1^0(\mu) + T_{j3}^* P_3^0(\mu)]\sin[\tfrac{2\pi}{365}(t-\phi_j)]. \tag{6.2}$$

Here μ is the sine of the latitude and P_n^0 are the Legendre functions normalized so that

$$\begin{aligned} &\int_{-1}^{1} P^2 d\mu = 2 \\ &P_1^0(\mu) = \sqrt{3}\,\mu \\ &P_2^0(\mu) = \tfrac{\sqrt{5}}{2}(\mu^2 - 1) \\ &P_3^0(\mu) = \tfrac{\sqrt{7}}{2}(5\mu^2 - 3) \end{aligned} \tag{6.3}$$

t is in days and is zero at the vernal equinox. ϕ_j is a mild time-lag introduced in the troposphere to account for delayed ocean warmth. Trenberth used the following values for his eight levels:

TABLE 6.1

Z_j	P_j	z_j(km)	h_j(day^{-1})	d_j	T^*_{j2}(deg)	T^*_{j1}(deg)	T^*_{j3}(deg)
.511	.60	4	0.080	21	-15.4	6.54	0
1.204	.30	9	0.059	21	-10.3	5.97	0
2.120	.12	15	0.019	0	- 2.24	8.96	1.70
3.219	.04	22	0.026	0	- 4.64	11.80	3.32
4.605	.01	30.5	0.050	0	- 5.39	14.00	4.57
6.214	.002	43	0.190	0	- 5.37	11.70	5.45
7.601	.0005	54	0.240	0	- 1.78	11.20	4.89
9.210	.0001	63	0.200	0	0	2.77	1.21

The values of h_j used in our model (which are given in the next few pages) are similar to those of Trenberth, in the troposphere particularly. The values of T^*, however, have been rederived using Newell et al. [1972: The energy balance of the global atmosphere, in The global circulation of the atmosphere, pp. 42-90, Royal Meteorological Society, London 257 pp.; and 1974: The general circulation of the tropical atmosphere, Vol. 2, The MIT Press, Cambridge, MA 371 pp.] values of atmospheric heating rates. Thus

$$T^* = \frac{1}{h}\left(\frac{q}{c_p}\right) + T_0. \qquad (6.4)$$

where q/c_p is obtained from Newell et al. and T_0 represents the observed temperature distribution.

We use

$$T_j^*(\mu,t) = T_{j2}^* P_2^0(\mu) + T_{j4}^* P_4^0(\mu) + [T_{j1}^* P_1^0(\mu) + T_{j3}^* P_3^0(\mu)] \cdot \sin\left[\frac{2\pi}{360}(t - \phi_j)\right] \quad (6.5)$$

where $T_{ji}^* = 1.1\ (a_{ji}^0 + \frac{1}{hj}\, b_{ji}^0)$,

$\phi_j = 30$ days,

and there are twelve 30 day months in the model.

The values of a_{ji}^0 and b_{ji}^0 are given in Table 6.2. The resulting values of T^* are similar to those used by Trenberth except for the inclusion of the $P_4^0(\mu)$ component.

TABLE 6.2: Zonal heating parameters

		(degrees)				(degrees/day)			
j	Z	a_1^0	a_2^0	a_3^0	a_4^0	b_1^0	b_2^0	b_3^0	b_4^0
32	0	(5.5	-11.5	0.5	-1.5	.20	.06	.08	-.24)
31	.405	4.5	-10.0	0.1	-0.8	.34	-.20	.15	-.25
30	.811	4.0	- 8.9	0.1	-0.3	.24	-.53	-.13	.28
29	1.216	3.7	- 7.5	0.2	0.1	.11	-.15	-.10	.29
28	1.622	2.9	0.0	1.3	-0.1	.07	-.11	-.05	.13
27	2.027	2.6	7.4	3.0	-2.3	.10	-.10	.00	.02
26	2.433	3.2	8.4	3.2	-3.0	.14	-.20	.02	-.02
25	2.838	4.4	4.6	3.3	-2.1	.17	-.20	.03	-.02
24	3.244	5.2	1.5	3.2	-1.4	.19	-.21	.04	.02
23	3.649	5.6	- 0.1	2.7	-0.8	.21	-.29	.02	.06
22	4.055	5.9	- 0.6	2.0	-0.6	.29	-.35	.00	.06
21	4.460	6.0	- 1.4	2.0	-0.5	.46	-.35	-.03	.02

In addition to latitudinal forcing, the lower troposphere in the model is forced non-zonally. This forcing is applied at the three lowest levels only (levels 29, 30 and 31) and is based on Katayama's calculations of tropospheric heating rates. The heating is applied at each of the levels in the ratio $P_j h_j$. Thus, most of this forcing occurs at 667 mb. Fitting Katayama's computations by $P_n^1(\mu)$ and $P_m^2(\mu)$ terms where n = 1, 2, 3, 4 and m = 2, 3, 4, 5, the heating may be divided into those terms which are even about the equator (the annual terms) and those which are odd (the seasonal terms). The even terms are found to be produced primarily by equatorial forcing whereas those which are odd are due to mid-latitude forcing. Since our model is quasi-geostrophic, it may not respond realistically to equatorial forcing. Although the even terms were included in the 6 wave version of the model (but excluded from Trenberth's model), they have been excluded from the 18 wave model. Early tests of this model produced excessive tropospheric kinetic energy; the parameter changes made to produce a more realistic simulation included the elimination of these "annual" terms. The seasonal terms are given by

$$T_j^* = \frac{P_j h_j}{31 \sum_{j=29} P_j h_j} \sin \frac{2\pi}{360} (t - \phi_j) \sum_{\substack{n=\ell+1, \\ \ell+3}} \sum_{\ell=1}^{2} (\tau c_n^\ell \cos \ell\lambda + \tau s_n^\ell \sin \ell\lambda) P_n^\ell(\mu) \qquad (6.6)$$

where λ is longitude. Values of τc_n^ℓ and τs_n^ℓ are given in Table 6.3

TABLE 6.3: Non-zonal tropospheric forcing

ℓ	n	τc_n^{ℓ}	τs_n^{ℓ}
1	2	1.12	8.05
1	4	-2.09	-1.48
2	3	-8.57	2.15
2	5	-1.23	2.14

In the stratosphere, Trenberth's formula empirically represents all of the main types of radiation effects:

a. Short wave absorption by ozone and oxygen (20 km and higher)

b. 9.6 micron absorption and emission by ozone (20-30 km)

c. Infra-red absorption and emission by CO_2 (all heights)

In our model we will explicitly compute radiation of type a, as described in Chapter 5. This means that Trenberth's formulation must be changed for Z higher than 20 km ($Z \geq 2.9$). Type c can be represented by a simple Newtonian law

$$\frac{\partial T}{\partial t} = - h(p)T \ . \qquad (6.7)$$

The first reported runs of the model (Cunnold et al., JAS, 32, 170-194, 1975) used values obtained by Dickinson (A method or parameterization for infra-red cooling between altitudes of 30 and 70 km, JGR, 78, 4451-4457, 1973). He obtained values of h(p) by careful line integration of the CO and O_3 bands for a standard atmosphere, followed by a similar computation in which T was varied slightly. (Physically, this is satisfactory for the circumstance of cooling to

space - it does not include, however, the major effect of b above, which comes from absorption of radiation emitted by the ground in the water-vapor window region). Dickinson found values as follows:

Z	h(day^{-1})
11.4	.016
10.0	.062
9.1	.125
8.7	.172
7.9	.200
7.4	.220
6.9	.212
6.1	.135
4.8	.080
3.9	.060

The values of h currently being used are given as h_1 in Table 6.4. Between Z = 4.8 and 8.7, they match Dickinson's values. They, however, exceed Dickinson's values above Z > 8.7 and are smaller at Z = 3.9. The higher values at high altitudes are supported by the work of Kuhn and London (J. Atmos. Sci., 1969) while the values at low altitude are consistent with the values of h given in Table 6.1. Arguments in support of the latter values are given in Phillips (Tropospheric and lower stratospheric heating, internal memo, June 28, 1973). The support is provided by the radiation calculations of Manabe and Strickler (J. Atmos. Sci., 21, 364, 1964) and by experience with numerical models of the troposphere (e.g., Bushby and Whitelam, QJRMS, 87, 374-392, 1961).

TABLE 6.4: Two profiles of Newtonian cooling efficient used in the model calculations.

Model level	Z	h_1 (day^{-1})	h_2 (day^{-1})
1	12.6	.06	.06
2	12.2	.08	.08
3	11.8	.09	.09
4	11.4	.10	.10
5	10.9	.11	.11
6	10.5	.13	.13
7	10.1	.14	.14
8	9.7	.15	.15
9	9.3	.16	.16
10	8.9	.17	.17
11	8.5	.19	.19
12	8.1	.20	.20
13	7.7	.21	.21
14	7.3	.21	.21
15	6.9	.19	.19
16	6.5	.17	.16
17	6.1	.14	.14
18	5.7	.12	.12
19	5.3	.11	.10
20	4.9	.09	.09
21	4.5	.07	.08
22	4.1	.06	.07
23	3.6	.04	.06
24	3.2	.03	.05
25	2.8	.02	.05
26	2.4	.02	.05
27	2.0	.02	.05
28	1.6	.03	.05
29	1.2	.05	.06
30	0.8	.07	.07
31	0.4	.10	.09
32	0.0	.14	.14

The formula used in the computations to generate the values of h_1 given in Table 6.4 is

$$h = 0.22 - 0.03\,(Z - 7.4) \qquad Z \geq 7.4$$

$$= 0.02 + 0.20\left\{\frac{Z - 2.5}{4.9}\right\}^{3/2} \qquad 7.4 \geq Z \geq 2.5$$

$$= 0.02 + 0.12\left\{\frac{2.5 - Z}{2.5}\right\}^{2} \qquad 2.5 \geq Z \geq 0 \quad .$$

Heating due to the 9.6 micron O_3 band has been computed by Dopplick (Ph.D. thesis, M.I.T., 1970) using typical observed values of O_3. It gives a heating rate more or less independent of season with a peak value of 1.1 deg day^{-1} at the poles, centered at an altitude of about 25 km ($Z = 3.5$). This may be represented most simply by

$$\frac{\partial T}{\partial t} = -\frac{0.8}{\sqrt{5}} P_2^0(\mu)\,[1 - (Z - 3.5)^2] \text{ deg/day} \qquad (6.8)$$

for $2.5 \leqq Z \leqq 4.5$ and zero for Z values outside this range. As such, this heating does not depend on O_3 or T. This is not too critical, however, since the physical dependence on T is primarily due to ocean surface and cloud top temperatures, and any moderate variations in O_3 from that used by Dopplick will mostly shift somewhat the height $Z = 3.5$ vertically (i.e., the existing O_3 is ample to absorb all this upwelling radiation).

We therefore use the following strategy for heating computations. Define

Method I.

a. Explicit computation of short wave heating

b. Infra-red cooling with the Newtonian cooling formula (6.7)

c. Formula (6.8) for O_3 window radiation for $2.5 \leqq Z \leqq 4.5$

Method II.

Trenberth's formulas

These methods are combined as follows for different height ranges. (Z = 2.5 and 4.5 corresponds roughly to heights of 17.5 and 30.3 km).

A. $Z > 4.5$: Only Method I.

B. $2.5 \leq Z \leq 4.5$: Weighted average of I and II as follows:

$$\left(\frac{Z - 2.5}{2}\right) \times \text{Method I} + \left(\frac{4.5 - Z}{2}\right) \times \text{Method II.}$$

C. $z \leq 2.5$: Only Method II.

7. Spectral form of the equations

We define spectral solutions at arbitrary level j in the form

$$\left.\begin{aligned} \psi_j &= \sum_\alpha \psi_{\alpha,j} Y_\alpha(\lambda,\mu) \\ \zeta_j &= \sum_\alpha \zeta_{\alpha,j} Y_\alpha(\lambda,\mu) \\ W_j &= \sum_\alpha W_{\alpha,j} Y_\alpha(\lambda,\mu) \\ T_j &= \sum_\alpha T_{\alpha,j} Y_\alpha(\lambda,\mu) \\ q_j &= \sum_\alpha q_{\alpha,j} Y_\alpha(\lambda,\mu) \end{aligned}\right\} , \tag{7.1}$$

and for the trace substance equation

$$\left.\begin{aligned} \chi_j &= \sum_\alpha \chi_{\alpha,j} Y_\alpha(\lambda,\mu) \\ G_j &= \sum_\alpha G_{\alpha,j} Y_\alpha(\lambda,\mu) \end{aligned}\right\} . \tag{7.2}$$

In terms of longitude (λ) and latitude (μ), we have defined members of the complete set of orthogonal spherical harmonics in (7.1) and (7.2) using

$$Y_\alpha(\lambda,\mu) = e^{i\ell_\alpha \lambda} P_\alpha(\mu) \tag{7.3}$$

with

$$\alpha = n_\alpha + i\ell_\alpha \tag{7.4}$$

denoting a vector index of planetary wave number ℓ_α and degree n_α. The $P_\alpha(\mu)$ are Legendre polynomials of rank and degree given by α. Normalization of the

spherical harmonics is such that integration over the unit spherical surface (s) yields the orthogonal property

$$\int_s Y_\alpha Y_\beta^* \, ds = 4\pi\delta_{\alpha,\beta} \quad . \tag{7.5}$$

Complex conjugate values are denoted by an asterisk. Another useful property of the set of spherical harmonics is that they satisfy the differential equation

$$\nabla^2 Y_\alpha = -c_\alpha Y_\alpha ; \; c_\alpha = n_\alpha(n_\alpha+1) \tag{7.6}$$

The complete set of orthonormal Legendre polynomials as used in (7.3) are defined such that

$$P_\alpha^* \equiv P_\alpha \tag{7.7}$$

and all P_α have been normalized such that

$$\int_{-1}^{+1} P_\alpha P_\beta \, d\mu = 2\delta_{\alpha,\beta} \tag{7.8}$$

We now want to substitute solutions (7.1) and (7.2) into the non-dimensional forms of our model equations, multiply through with a member of the orthogonal set (say, Y_γ^*), and integrate the resulting relationships over the unit sphere. Application of this procedure to the vorticity equation (3.9), for example, yields the desired spectral form of this equation,

$$\frac{d\zeta_{\gamma,j}}{dt} = -i\ell_\gamma\psi_{\gamma,j} - A_{\gamma,j} + \frac{D_\gamma}{c_{\gamma-\varepsilon}}\left[(\frac{r}{r-1})W_{\gamma-\varepsilon,j+1} - \right.$$

$$\left. -(\frac{1}{r-1})W_{\gamma-\varepsilon,j}\right] - \frac{E_\gamma}{c_{\gamma+\varepsilon}}\left[(\frac{r}{r-1})W_{\gamma+\varepsilon,j+1} - \right. \qquad (7.9)$$

$$\left. -(\frac{1}{r-1})W_{\gamma+\varepsilon,j}\right] + (\frac{r}{r-1})F_{\gamma,j+1} - (\frac{1}{r-1})F_{\gamma,j} +$$

$$(2-C_r)A_{H)j}\,\zeta_{\gamma,j}$$

in which, over the unit spherical surface s,

$$\left.\begin{aligned}
&\frac{d\zeta_{\gamma,j}}{dt} = \frac{1}{4\pi}\int_s \frac{\partial\zeta_j}{\partial t}\,Y^*_\gamma\,ds \\
&i\ell_\gamma\psi_{\gamma,j} = \frac{1}{4\pi}\int_s J(\psi_j,\mu)Y^*_\gamma ds = \frac{1}{4\pi}\int_s \frac{\partial\psi_j}{\partial\lambda}Y^*_\gamma ds \\
&A_{\gamma,j} = \frac{1}{4\pi}\int_s J(\psi_j,\zeta_j)Y^*_\gamma ds \quad \text{(See Appendix A)} \\
&\frac{D_\gamma}{c_{\gamma-\varepsilon}}W_{\gamma-\varepsilon,j} - \frac{E_\gamma}{c_{\gamma+\varepsilon}}W_{\gamma+\varepsilon,j} = -\frac{1}{4\pi}\int_s [\nabla\cdot\mu\nabla L(W_j)]Y^*_\gamma ds \quad \text{(See Appendix B)} \\
&F_{\gamma,j} = \frac{1}{4\pi}\int_s F_j Y^*_\gamma ds \\
&(2-c_\gamma)A_{H)j}\zeta_{\gamma,j} = \frac{1}{4\pi}\int_s A_{H)j}[\nabla^4\psi_j + 2\nabla^2\psi_j]Y^*_\gamma ds
\end{aligned}\right\} \qquad (7.10)$$

Similarly, the thermodynamic energy equation (3.19), the trace substance equation (3.21), and the thermal wind relationship (3.18) reduce to the spectral forms

$$
\begin{aligned}
\frac{dT_{\gamma,j}}{dt} &= -B_{\gamma,j} - S_j W_{\gamma,j} - A_{H)j}\, c_\gamma T_{\gamma,j} + \left[\frac{R}{C_p 8\Omega^3 a^2}\right] q_{\gamma,j} \\
\frac{d\chi_{\gamma,j}}{dt} &= -B^{(\chi)}_{\gamma,j} - \left(\frac{d\bar{\chi}}{dZ}\right) W_{\gamma,j} + \left(\frac{r}{r-1}\right) G_{\gamma,j} - \left(\frac{1}{r-1}\right) G_{\gamma,j} - \\
&\quad -A_{H)j}\, c_\gamma \chi_{\gamma,j} + \frac{1}{4\pi}\int_s \frac{1}{2\Omega}\left[\frac{1}{n_m}\left(\frac{dn}{dt}\right)_c\right]_j Y^*_\gamma ds \\
\nabla Z\, c_\gamma T_{\gamma,j} &= -D_\gamma\left(\psi_{\gamma-\varepsilon,j-1} - \psi_{\gamma-\varepsilon,j}\right) + E\left(\psi_{\gamma+\varepsilon,j-1} - \psi_{\gamma+\varepsilon,j}\right)
\end{aligned}
\qquad (7.11)
$$

where, for example,

$$
\begin{aligned}
\frac{dT_{\gamma,j}}{dt} &= \frac{1}{4\pi}\int_s \frac{\partial T_j}{\partial t} Y^*_\gamma ds \\
\frac{d\chi_{\gamma,j}}{dt} &= \frac{1}{4\pi}\int_s \frac{d\chi_j}{dt} Y^*_\gamma ds \\
c_\gamma T_{\gamma,j} &= \frac{1}{4\pi}\int_s \left(-\nabla^2 T_j\right) Y^*_\gamma ds \\
B_{\gamma,j} &= \frac{1}{8\pi}\int_s J\left(\psi_j + \psi_{j-1}, T_j\right) Y^*_\gamma ds \quad \text{(See Appendix A)} \\
B^{(\chi)}_{\gamma,j} &= \frac{1}{8\pi}\int_s J\left(\psi_j + \psi_{j-1}, \chi_j\right) Y^*_\gamma ds \quad \text{(See Appendix A)} \\
D_\gamma \psi_{\gamma-\varepsilon,j} - E_\gamma \psi_{\gamma+\varepsilon,j} &= -\frac{1}{4\pi}\int_s \left[\nabla\cdot\mu\nabla\psi_j\right] Y^*_\gamma ds \quad \text{(See Appendix B)}
\end{aligned}
\qquad (7.12)
$$

In addition, we want to determine the spectral form of (1.6) relating the verti-

cal component of relative vorticity (ζ) and the streamfunction (ψ). It can be shown that

$$\zeta_{\gamma,j} = -c_\gamma \psi_{\gamma,j} \tag{7.13}$$

or

$$\psi_{\gamma,j} = -\frac{\zeta_{\gamma,j}}{c_\gamma} \tag{7.14}$$

provided that in (6.14) we stipulate $\gamma \neq 0+i0$ (i.e., $c_\gamma \neq 0$).

The spectral relationships (7.9), (7.11), and (7.13) [or (7.14)] along with definitions (7.10) and (7.12) form a complete set of equations for solution. However, it is not convenient to attempt to integrate the model in this form as there is no explicit relationship determining the vertical velocity field represented by W. In order to define W, we want to alter the thermal wind relationship in (7.11). This development is contained in the next section. Furthermore, specification of the truncation limits to be used for series solutions (7.1) and (7.2) have not yet been established and will be discussed in a later section.

8. Determination of W in the dynamic equations

In order to obtain an explicit description of the vertical motion fields in our model atmosphere, we insert (7.14) into the thermal wind equation of (7.11) and differentiate w.r.t. time to get

$$\Delta Z\, c_\gamma \frac{dT_{\gamma,j}}{dt} = \frac{D_\gamma}{c_{\gamma-\varepsilon}} \left[\frac{d\zeta_{\gamma-\varepsilon,j-1}}{dt} - \frac{d\zeta_{\gamma-\varepsilon,j}}{dt}\right] - \frac{E_\gamma}{c_{\gamma+\varepsilon}} \left[\frac{d\zeta_{\gamma+\varepsilon,j-1}}{dt} - \frac{d\zeta_{\gamma+\varepsilon,j}}{dt}\right] \tag{8.1}$$

for all levels $j = 2,3, \ldots, J-1$. We note that (8.1) does not apply for the cases $\gamma = 0+i0$. Furthermore, for notational purposes, we will stipulate that in (8.1) and all future relationships, terms which require $\gamma-\varepsilon = 0+i0$ or $n_{\gamma-\varepsilon} < \ell_{\gamma-\varepsilon}$ do not exist. This applies equally to cases in which $\gamma+\varepsilon$ is not contained within the specified model truncation limits.

Let us now define

$$\left.\begin{aligned} a_{\gamma,j} \equiv & - i\ell_\gamma(\psi_{\gamma,j-1} - \psi_{\gamma,j}) - A_{\gamma,j-1} + A_{\gamma,j} - \\ & - \left(\frac{1}{r-1}\right)F_{\gamma,j-1} + \left(\frac{r+1}{r-1}\right)F_{\gamma,j} - \left(\frac{r}{r-1}\right)F_{\gamma,j+1} + \\ & A_{H)j}\,(2-c_\gamma)\,(\zeta_{\gamma,j-1} - \zeta_{\gamma,j}) \\ b_{\gamma,j} \equiv & - B_{\gamma,j} - A_{H)j}\, c_\gamma T_{\gamma,j} + \left[\frac{R}{C_p 8\Omega^3 a^2}\right] q_{\gamma,j} \end{aligned}\right\} \tag{8.2}$$

such that using (7.9) we can write

$$\frac{d\zeta_{\gamma,j-1}}{dt} - \frac{d\zeta_{\gamma,j}}{dt} = a_{\gamma,j} - \frac{1}{(r-1)} \frac{D_\gamma}{c_{\gamma-\varepsilon}} [W_{\gamma-\varepsilon,j-1} - (r+1)W_{\gamma-\varepsilon,j} +$$

$$+ rW_{\gamma-\varepsilon,j+1}] + \frac{1}{(r-1)} \frac{E_\gamma}{c_{\gamma+\varepsilon}} [W_{\gamma+\varepsilon,j-1} - \tag{8.3}$$

$$- (r+1)W_{\gamma+\varepsilon,j} + rW_{\gamma+\varepsilon,j+1}]$$

and, the thermodynamic energy equation of (7.11) reduces to

$$\frac{dT_{\gamma,j}}{dt} = b_{\gamma,j} - S_j W_{\gamma,j} \quad . \tag{8.4}$$

Inserting solutions (8.3) and (8.4) into (8.1) has the effect of eliminating the time dependence of (8.1) and at any given time we have

$$\Delta Z\, c_\gamma b_{\gamma,j} - \Delta Z\, c_\gamma S_j W_{\gamma,j} = \frac{D_\gamma}{c_{\gamma-\varepsilon}} a_{\gamma-\varepsilon,j} - \frac{E_\gamma}{c_{\gamma+\varepsilon}} a_{\gamma+\varepsilon,j} -$$

$$- \frac{1}{(r-1)} \frac{D_{\gamma-\varepsilon} D_\gamma}{c_{\gamma-2\varepsilon} c_{\gamma-\varepsilon}} [W_{\gamma-2\varepsilon,j-1} - (r+1)W_{\gamma-2\varepsilon,j} + rW_{\gamma-2\varepsilon,j+1}] +$$

$$+ \frac{1}{(r-1)} \left[\frac{E_{\gamma-\varepsilon} D_\gamma}{c_{\gamma-\varepsilon} c_\gamma} + \frac{E_\gamma D_{\gamma+\varepsilon}}{c_\gamma c_{\gamma+\varepsilon}} \right] [W_{\gamma,j-1} - (r+1)W_{\gamma,j} + rW_{\gamma,j+1}] -$$

$$- \frac{1}{(r-1)} \frac{E_\gamma E_{\gamma+\varepsilon}}{c_{\gamma+\varepsilon} c_{\gamma+2\varepsilon}} [W_{\gamma+2\varepsilon,j-1} - (r+1)W_{\gamma+2\varepsilon,j} + rW_{\gamma+2\varepsilon,j+1}]$$

or, if we define

$$
\begin{aligned}
\pi_{\gamma,j} &\equiv (r-1)\left[\frac{D_\gamma}{c_{\gamma-\varepsilon}c_\gamma}\, a_{\gamma-\varepsilon,j} - \frac{E_\gamma}{c_\gamma c_{\gamma+\varepsilon}}\, a_{\gamma+\varepsilon,j} - \Delta Z\; b_{\gamma,j}\right] \\
f_\gamma^{(1)} &\equiv \frac{D_{\gamma-\varepsilon}D_\gamma}{c_{\gamma-2\varepsilon}c_{\gamma-\varepsilon}c_\gamma} \\
f_\gamma^{(2)} &\equiv -\frac{1}{c_\gamma^2}\left[\frac{E_{\gamma-\varepsilon}D_\gamma}{c_{\gamma-\varepsilon}} + \frac{E_\gamma D_{\gamma+\varepsilon}}{c_{\gamma+\varepsilon}}\right] \\
f_\gamma^{(3)} &\equiv \frac{E_\gamma E_{\gamma+\varepsilon}}{c_\gamma c_{\gamma+\varepsilon}c_{\gamma+2}} \\
\sigma_j &\equiv (r-1)\Delta Z\; S_j
\end{aligned}
\qquad (8.5)
$$

the W-equation can be compacted to

$$
\begin{aligned}
&[f_\gamma^{(1)}W_{\gamma-2\varepsilon,j-1} + f_\gamma^{(2)}W_{\gamma,j-1} + f_\gamma^{(3)}W_{\gamma+2\varepsilon,j-1}] - \\
&- (r+1)\,[f_\gamma^{(1)}W_{\gamma-2\varepsilon,j} + f_\gamma^{(2)}W_{\gamma,j} + f_\gamma^{(3)}W_{\gamma+2\varepsilon,j}] + \\
&+r[f_\gamma^{(1)}W_{\gamma-2\varepsilon,j+1} + f_\gamma^{(2)}W_{\gamma,j+1} + f_\gamma^{(3)}W_{\gamma+2\varepsilon,j+1}] - \\
&- \sigma_j W_{\gamma,j} = \pi_{\gamma,j}
\end{aligned}
\qquad (8.6)
$$

in which from (1.17) we represent the boundary conditions as

$$
\begin{aligned}
W_{\gamma,1} &= 0 \\
W_{\gamma,J} &= H_\gamma \\
H_\gamma &\equiv \frac{1}{4\pi}\int_s J(\Psi_{J-1}, h/H_o)Y_\gamma^*\, ds
\end{aligned}
\qquad (8.7)
$$

To prepare (8.6) for inversion we want to take note of certain properties of the equations in order to reduce the calculation to a finite set of simple matrix solutions. Inspection of (8.6) shows that the equations uncouple according to planetary wave numbers, ℓ_γ. In addition, within each planetary wave the equations contain two independent sets; one of even vector elements ($n_\gamma + \ell_\gamma$ all even) and the others of odd vector elements ($n_\gamma + \ell_\gamma$ all odd). Thus, to facilitate ease of notation, let us define some new sets of indices to be applied to (8.6) by first denoting a maximum planetary wave number, L, for a given spectral truncation as

$$L = \ell_\gamma)_{max} \tag{8.8}$$

so that we can designate K independent sets of matrix equations using index k where

$$k = 1, 2, 3, \ldots, K; \; K = 2(L+1). \tag{8.9}$$

For a given matrix set we will determine k by designating

$$k = \begin{cases} 2\ell_\gamma + 1 \text{ for even vector sets} \\ 2(\ell_\gamma + 1) \text{ for odd vector sets} \end{cases} . \tag{8.10}$$

Furthermore, within each of the K matrix equation sets it is useful to designate an element index, b_k, where

$$b_k = 1, 2, 3, \ldots, B_k \; . \tag{8.11}$$

Thus, for a given matrix set designated by the subscript k we devise the b_k indices as follows:

(1) For k odd (even vectors) let

$$N_k = n_k)_{max} \tag{8.12}$$

for which we consider only n_k from the set $n_k + \ell_k$ even. Then the value for an individual b_k is determined from

$$\left.\begin{aligned} b_k &= \frac{n_k - \ell_k + 2}{2} - \delta_{\ell_k,0} \\ B_k &= \frac{N_k - \ell_k + 2}{2} - \delta_{\ell_k,0} \end{aligned}\right\} \tag{8.13}$$

where we ignore values of b_k outside the range indicated in (8.11); i.e., when $k = 1$, $n_1 = 0$, and $\ell_1 = 0$ we do not include the value $b_1 = 0$ which designates the nonallowable equation of (8.1) in which $\gamma = 0+i0$ [see comments following (8.1)].

Similarily,

(2) For k even (odd vectors) let

$$N_k = n_k)_{max} \tag{8.14}$$

in which here we consider only n_k from the set $n_k + \ell_k$ odd. Then, we have

$$\left.\begin{aligned} b_k &= \frac{n_k - \ell_k + 1}{2} \\ B_k &= \frac{N_k - \ell_k + 1}{2} \end{aligned}\right\} \tag{8.15}$$

At this point we want to note an additional property inherent in the spectral W-equations represented by (8.6). That is, from definitions contained in

(8.5) and Appendix B we can show that for any given k,

$$f^{(3)}_{b_k} = \frac{E_{\gamma_k} \; E_{\gamma_k \mp \varepsilon}}{c_{\gamma_k} \; c_{\gamma_k \mp \varepsilon} \; c_{\gamma_k \mp 2\varepsilon}}$$

$$\equiv \frac{D_{\gamma_k \mp \varepsilon} \; D_{\gamma_k \mp 2\varepsilon}}{c_{\gamma_k} \; c_{\gamma_k \mp \varepsilon} \; c_{\gamma_k \mp 2\varepsilon}} \equiv f^{(1)}_{b_k \mp 1} \tag{8.16}$$

We are now prepared to convert (8.6) to matrix form. To do this we first define tridiagonal matrices $\mathcal{D}_k$ as

$$\mathcal{D}_k = \begin{bmatrix} f^{(2)}_1 & f^{(3)}_1 & 0 \cdots\cdots 0 \\ f^{(3)}_1 & f^{(2)}_2 & f^{(3)}_2 \\ \ddots & \ddots & \ddots \\ 0 & f^{(3)}_{b_k-1} & f^{(2)}_{b_k} \quad f^{(3)}_{b_k} \\ \vdots & \ddots & \ddots \quad \ddots \\ \vdots & & \ddots \quad \ddots \quad \ddots \\ \vdots & & \ddots \quad \ddots \quad \ddots \\ 0 \cdots\cdots\cdots & & f^{(3)}_{B_k-1} \quad f^{(2)}_{B_k} \end{bmatrix}_k \tag{8.17}$$

where we have made use of (8.8) - (8.16). We note from (8.17) that not only is each $\mathcal{D}_k$ <u>tridiagonal</u> but it is also symmetric. In addition, it can be shown that every principle minor determinate of $\mathcal{D}_k$ is <u>positive</u> and thus $\mathcal{D}_k$ can be said to be <u>positive definite</u>. These properties will be discussed in more detail below.

To complete the conversion of (8.6) to matrix form we define vectors

$$W_{k,j} = \begin{pmatrix} W_{1,j} \\ W_{2,j} \\ \vdots \\ W_{b_k,j} \\ \vdots \\ W_{B_k,j} \end{pmatrix}_k ; \quad R_{k,j} = \begin{pmatrix} r_{1,j} \\ r_{2,j} \\ \vdots \\ r_{b_k,j} \\ \vdots \\ r_{B_k,j} \end{pmatrix}_k \tag{8.18}$$

such that (8.6) can be written in the matrix form

$$\begin{aligned} &\mathcal{D}_k W_{k,j-1} - (r+1)\mathcal{D}_k W_{k,j} + r\mathcal{D}_k W_{k,j+1} - \sigma_j W_{k,j} = R_{k,j} \quad ; \\ &\quad j = 2, 3, 4, \ldots, J-1 \text{ for each } k = 1, 2, 3, \ldots, K \end{aligned} \tag{8.19}$$

We wish to modify (8.19) through diagonalization of each $\mathcal{D}_k$. However, since each tridiagonal $\mathcal{D}_k$ is real, symmetric and positive definite, we know that all eigenvalues of $\mathcal{D}_k$ are real and positive. Also, the sets of eigenvectors associated with these eigenvalues are orthonormal. Thus, if $\mathcal{D}_k$ is an MxM matrix, there exists a set of real positive eigenvalues $(\lambda_k)_p$ with p = 1, 2, 3, ..., M associated with $\mathcal{D}_k$ and M sets of orthonormal eigenvectors $q_{p,s}$ with s = 1, 2, 3, ..., M. If we let Q_k represent the matrix of eigenvectors associated with the the set $(\lambda_k)_p$ and matrix $\mathcal{D}_k$, we have

$$Q_k = \begin{pmatrix} q_{11} & q_{12} & \cdots & q_{1s} & \cdots & q_{1m} \\ q_{21} & q_{22} & \cdots & q_{2s} & \cdots & q_{2m} \\ \vdots & \vdots & & \vdots & & \vdots \\ q_{p1} & q_{p2} & \cdots & q_{ps} & \cdots & q_{pm} \\ \vdots & \vdots & & \vdots & & \vdots \\ q_{m1} & q_{m2} & \cdots & q_{ms} & \cdots & q_{mm} \end{pmatrix}_k \tag{8.20}$$

such that

$$Q_k\tilde{Q}_k = \tilde{Q}_kQ_k = I \tag{8.21}$$

where I is the unit matrix and $(\tilde{\ })$ denotes transposition. Define

$$\Lambda_k = \begin{bmatrix} (\lambda_k)_1 & 0 & \cdots & 0 \\ 0 & (\lambda_k)_2 & & \vdots \\ \vdots & & (\lambda_k)_p & \vdots \\ 0 & \cdots & \cdots & (\lambda_k)_m \end{bmatrix} \tag{8.22}$$

were then we know

$$\left.\begin{aligned} \mathcal{D}_kQ_k &= Q_k\Lambda_k \\ \text{and} \\ \tilde{Q}_k\mathcal{D}_kQ_k &= \tilde{Q}_kQ_k\Lambda_k = \Lambda_k \end{aligned}\right\} . \tag{8.23}$$

We now want to expand the vector $W_{k,j}$ in (8.19) in the form

$$W_{k,j} = Q_kV_{k,j} \; ; \; V_{k,j} = \tilde{Q}_kW_{k,j} \tag{8.24}$$

where we note that $V_{k,j}$ is also a vector.

Inserting solutions (8.24) into (8.19) and multiplying through with $\tilde{Q}_k$ gives

$$\tilde{Q}_k\mathcal{D}_kQ_kV_{k,j-1} - (r+1)\tilde{Q}_k\mathcal{D}_kQ_kV_{k,j} + r\tilde{Q}_k\mathcal{D}_kQ_kV_{k,j+1} - \\ - \sigma_j\tilde{Q}_kQ_kV_{k,j} = \tilde{Q}_kR_{k,j}$$

or, from (8.23), we can write

$$\Lambda_k V_{k,j-1} - [(r+1)\,\Lambda_k + \sigma_j]\,V_{k,j} + r\Lambda_k V_{k,j+1} = \tilde{Q}_k R_{k,j} \tag{8.25}$$

Now, we know that there exists an inverse

$$\Lambda_k^{-1} = \begin{bmatrix} 1/(\lambda_k)_1 & 0 & \cdots & 0 \\ 0 & 1/(\lambda_k)_2 & & \vdots \\ \vdots & & \ddots & \vdots \\ & & 1/(\lambda_k)_p & \\ 0 & \cdots & & 1/(\lambda_k)_m \end{bmatrix} \tag{8.26}$$

such that

$$\Lambda_k^{-1}\Lambda_k = I\ . \tag{8.27}$$

Thus, if we multiply (8.25) through with Λ_k^{-1}, (8.25) reduces to the form

$$V_{k,j-1} - [(r+1)I + \sigma_j\Lambda_k^{-1}]\,V_{k,j} + rV_{k,j+1} = \Lambda_k^{-1}\tilde{Q}_k R_{k,j} \tag{8.28}$$

where for each k = 1, 2, 3, ..., K we have j = 2, 3, 4, ..., j-1. We now let

$$S_{k,j} \equiv -[(r+1)I + \sigma_j\Lambda_k^{-1}]$$

and

$$R_{k,j} \equiv \begin{cases} \Lambda_k^{-1}\tilde{Q}_k R_{k,2} - V_{k,1} & (\text{for } j = 2) \\ \Lambda_k^{-1}\tilde{Q}_k R_{k,j} & (\text{for } 3 \le j \le J-2) \\ \Lambda_k^{-1}\tilde{Q}_k R_{k,J-1} - rV_{k,j} & (\text{for } j = J-1) \end{cases} \tag{8.29}$$

Using (8.29), (8.28) transforms to the set

$$\left.\begin{aligned} S_{k,2}V_{k,2} + r\,V_{k,3} &= R_{k,2} && \text{(for } j = 2\text{)} \\ V_{k,j-1} + S_{k,j}V_{k,j} + r\,V_{k,j+1} &= R_{k,j} && \text{(} 3 \le j \le J-2\text{)} \\ V_{k,J-2} + S_{k,J-1}V_{k,J-1} &= R_{k,J-1} && \text{(for } j = J-1\text{)} \end{aligned}\right\} \qquad (8.30)$$

in which from (8.24) and the boundary conditions of (8.7) we see that in (8.29)

$$\left.\begin{aligned} V_{k,1} &= 0 \\ V_{k,J} &= \tilde{Q}_k W_{k,J} \equiv \tilde{Q}_k H_k \end{aligned}\right\} \quad . \qquad (8.31)$$

We see that for each k the system (8.30) is tridiagonal in j and thus submits readily to solution provided certain provisions are met (see Appendix C for details). Briefly, to invert (8.30) we first define

$$\left.\begin{aligned} u_{k,2} &\equiv S_{k,2}^{-1} && \text{(for } j = 2\text{)} \\ u_{k,j} &\equiv (S_{k,j} - r\,u_{k,j-1})^{-1} && \text{(for } 3 \le j \le J-1\text{)} \\ v_{k,j} &\equiv -\,r\,u_{k,j} && \text{(} 2 \le j \le J-1\text{)} \end{aligned}\right\} \qquad (8.32)$$

and then let

$$\left.\begin{aligned} y_{k,2} &= u_{k,2}\,R_{k,2} && \text{(for } j = 2\text{)} \\ y_{k,j} &= u_{k,j}\,(R_{k,j} - y_{k,j-1}) && \text{(for } 3 \le j \le J-1\text{)} \end{aligned}\right\} \quad . \qquad (8.33)$$

Solutions to (8.30) thus appear as

$$\left.\begin{aligned} V_{k,J-1} &= y_{k,J-1} \qquad (\text{for } j = J-1) \\ V_{k,j} &= v_{k,j} V_{k,j+1} + y_{k,j} \quad (\text{for } j = J-2,\ J-3,\ \ldots,\ 2) \end{aligned}\right\} \tag{8.34}$$

provided all $u_{k,j}$ in (8.23) exist and are finite. Vectors $W_{k,j}$ are then obtained from (8.24).

Appendix A. Evaluation of the nonlinear Jacobian terms using transformed fields.

On the unit sphere, the Jacobian of arbitrary horizontal global scalers A and B is given by

$$J(A,B) = \frac{\partial A}{\partial \lambda}\frac{\partial B}{\partial \mu} - \frac{\partial A}{\partial \mu}\frac{\partial B}{\partial \lambda} \tag{A.1}$$

where λ is longitude and μ is the sine of latitude. Expanding A and B in terms of spherical harmonics, we have

$$\begin{aligned} A &= \sum_{\alpha} a_{\alpha} Y_{\alpha}(\lambda,\mu) \\ B &= \sum_{\alpha} b_{\alpha} Y_{\alpha}(\lambda,\mu) \\ \alpha &= n_{\alpha} + i\ell_{\alpha} \end{aligned} \tag{A.2}$$

in which the special properties of the orthonomal spherical function $Y_{\alpha}(\lambda,\mu)$ are outlined in (7.3) - (7.8).

Rather than evaluate the Jacobian terms using the interaction coefficient methodology applied in the past for our lower order models, we will transform the terms in (A.1) to a special grid system devised to permit exact Gaussian guadrature integration of the nonlinear Jacobian terms. Details of this numerical procedures to be used in this process are contained in Eliasen et al., (1970). Briefly, however, we can assert that the selected grid system must be located on latitudes which form the "zeros" of the "highest order plus 1" Legendre polynomial contained in the Jacobian term for the particular truncation chosen. In the case of triangular spectral truncations (which we are currently using), we know that the number of the "Gaussian" latitudes needed, K_{max}, is given by

$$K_{max} = 1.5\,\ell_{max} + 1\,, \tag{A.3}$$

where ℓ_{max} is the maximum longitudinal wave number allowed. Thus, for a truncation triangle which contains planetary waves, 0 - 18, the formula requires that 28 latitudes be used to represent the minimum horizontal grid and that the latitudes are to be located on the zeros of the Legendre polynomial P_0^{28}. A similar procedure is used to specify the longitudinal grid points.

To evaluate (A.1) using the transform technique, we first define

$$\begin{aligned} M &= \frac{\partial A}{\partial \lambda} = \sum_{\alpha} i\ell_{\alpha} a_{\alpha} Y_{\alpha}(\lambda,\mu) \\ N &= \frac{\partial B}{\partial \mu} = \sum_{\alpha} b_{\alpha} e^{i\ell_{\alpha}\lambda} \frac{dP_{\alpha}(\mu)}{d\mu} \\ P &= \frac{\partial A}{\partial \mu} = \sum_{\alpha} a_{\alpha} e^{i\ell_{\alpha}\lambda} \frac{dP_{\alpha}(\mu)}{d\mu} \\ Q &= \frac{\partial B}{\partial \lambda} = \sum_{\alpha} i\ell_{\alpha} b_{\alpha} Y_{\alpha}(\lambda,\mu) \end{aligned} \tag{A.4}$$

where then (A.1) becomes

$$J(A,B) = MxN - PxQ\,. \tag{A.5}$$

The quantities M, N, P, Q are evaluated on the Gaussian grid by performing the sums indicated in (A.4) for each grid point. Details of the numerical methodology used for these transforms are given in Appendix E. The indicated products and differences indicated in (A.5) are performed at each grid point and the resulting Jacobian field is transformed back to the spectral domain and truncated to conform with the resolutions of the A and B spectrums.

Reference

Eliasen, E., B. Mackenhauer and E. Rasmussen, 1970: On a numerical method for integration of the hydrodynamical equations with a spectral representation of the horizontal fields. Report No. 2, Institut for Teoretisk Meteorologi, Kobenhavns Universitet, 37 pp.

Appendix B. Spectral representation of divergence terms of the general form $\nabla \cdot \mu\nabla A$.

In terms of spherical operators on the unit sphere in which λ is longitude and μ is the sine of latitude we have

$$\begin{aligned} \nabla \cdot \mu\nabla A &= \nabla\mu \cdot \nabla A + \mu\nabla^2 A \\ &= (1-\mu^2)\,\frac{\partial A}{\partial \mu} + \mu\nabla^2 A \end{aligned} \tag{B.1}$$

in which A is an arbitrary horizontal global scalar expandable in the form

$$A = \sum_{\alpha} a_\alpha Y_\alpha(\lambda,\mu) \quad . \tag{B.2}$$

Properties of the orthonormal spherical functions $Y_\alpha(\lambda,\mu)$ are outlined in (7.3) - (7.8). Insertion of solutions (B.2) into (B.1) yields

$$\left.\begin{aligned} \nabla \cdot \mu\nabla A &= (1-\mu^2)\sum_{\alpha} a_\alpha e^{i\ell_\alpha\lambda}\,\frac{dP_\alpha(\mu)}{d\mu} - \mu\sum_{\alpha} c_\alpha a_\alpha e^{i\ell\alpha\lambda}\,P_\alpha(\mu) \\ &= \sum_{\alpha} a_\alpha e^{i\ell_\alpha\lambda}\left[(1-\mu^2)\frac{dP_\alpha}{d\mu} - \mu c_\alpha P_\alpha\right], \\ c_\alpha &= n_\alpha(n_\alpha+1) \end{aligned}\right\} \quad . \tag{B.3}$$

But, if we define

$$\begin{aligned} N_\alpha &= \left[\frac{(2n_\alpha+1)(n_\alpha-\ell_\alpha)!}{(n_\alpha+\ell_\alpha)!}\right]^{1/2} \\ \varepsilon &= 1 + i0 \end{aligned} \tag{B.4}$$

then we know from the Legendre differential and recurrence relations (for example, see Jahnke and Emde, 1945) that

$$\left.\begin{aligned}(1-\mu^2)\frac{dP_\alpha}{d\mu} &= -n_\alpha \mu P_\alpha + (n_\alpha+\ell_\alpha)\frac{N_\alpha}{N_{\alpha-\varepsilon}} P_{\alpha-\varepsilon} \\ \text{and} \\ \mu P_\alpha &= \frac{(n_\alpha-\ell_\alpha+1)}{(2n_\alpha+1)} \frac{N_\alpha}{N_{\alpha+\varepsilon}} P_{\alpha+\varepsilon} + \frac{(n_\alpha+\ell_\alpha)}{(2n_\alpha+1)} \frac{N_\alpha}{N_{\alpha-\varepsilon}} P_{\alpha-\varepsilon}\end{aligned}\right\} . \quad (B.5)$$

Then, using (B.5), we can show that

$$(1-\mu^2)\frac{dP_\alpha}{d\mu} - \mu c_\alpha P_\alpha = \frac{(1-n_\alpha^2)(n_\alpha+\ell_\alpha)}{(2n_\alpha+1)} \frac{N_\alpha}{N_{\alpha-\varepsilon}} P_{\alpha-\varepsilon} - \frac{n_\alpha(n_\alpha+2)(n_\alpha-\ell_\alpha+1)}{(2n_\alpha+1)} \frac{N_\alpha}{N_{\alpha+\varepsilon}} P_{\alpha+\varepsilon}. \quad (B.6)$$

We now insert (B.6) into (B.3), multiply through using $Y_\gamma^* /4\pi$, and integrate over the unit sphere to get

$$\frac{1}{4\pi}\int_0^{2\pi}\int_{-1}^{1}(\nabla\cdot\mu\nabla A)Y_\gamma^* d\mu d\lambda = \sum_{\substack{\alpha \\ \ell_\alpha=\ell_\gamma}} a_\alpha\left[\frac{(1-n_\alpha^2)(n_\alpha+\ell_\alpha)}{(2n_\alpha+1)} \frac{N_\alpha}{N_{\alpha-\varepsilon}}\right]\frac{1}{2}\int_{-1}^{1} P_{\alpha-\varepsilon}P_\gamma d\mu -$$

$$- \sum_{\substack{\alpha \\ \ell_\alpha=\ell_\gamma}} a_\alpha\left[\frac{n_\alpha(n_\alpha+2)(n_\alpha-\ell_\alpha+1)}{(2n_\alpha+1)} \frac{N_\alpha}{N_{\alpha+1}}\right]\frac{1}{2}\int_{-1}^{1} P_{\alpha+\varepsilon}P_\gamma d\mu$$

$$= (1-n_\gamma^2)\left[\frac{(n_\gamma+\ell_\gamma)(n_\gamma-\ell_\gamma)}{(2n_\gamma-1)(2n_\gamma+1)}\right]^{1/2} a_{\gamma-\varepsilon} -$$

$$- n_\gamma(n_\gamma+2)\left[\frac{(n_\gamma+\ell_\gamma+1)(n_\gamma-\ell_\gamma+1)}{(2n_\gamma+1)(2n_\gamma+3)}\right] a_{\gamma+\varepsilon}$$

$$= D_\gamma a_{\gamma-\varepsilon} - E_\gamma a_{\gamma+\varepsilon} \qquad (B.7)$$

where we have defined

$$D_\gamma \equiv (1-n_\gamma^2)\left[\frac{(n_\gamma+\ell_\gamma)(n_\gamma-\ell_\gamma)}{(2n_\gamma-1)(2n_\gamma+1)}\right]^{1/2}$$

$$E_\gamma \equiv n_\gamma(n_\gamma+2)\left[\frac{(n_\gamma+\ell_\gamma+1)(n_\gamma-\ell_\gamma+1)}{(2n_\gamma+1)(2n_\gamma+3)}\right]^{1/2} \qquad (B.8)$$

A special case of (B.7) occurs when we consider scalar B in which

$$B = \nabla^2 A \qquad (B.9)$$

where similar to (B.2) we can expand B in the form

$$B = \sum_\alpha b_\alpha Y_\alpha(\lambda,\mu). \qquad (B.10)$$

Then, from (7.6), we know that

$$b_\alpha = -c_\alpha a_\alpha \qquad (B.11)$$

and, in terms of coefficients b_α, (B.7) becomes

$$\frac{1}{4\pi}\int_0^{2\pi}\int_{-1}^{1}(\nabla\cdot\mu\nabla A)Y_\gamma^* d\mu d\lambda = -\frac{D_\gamma}{c_{\gamma-\varepsilon}} b_{\gamma-\varepsilon} + \frac{E_\gamma}{c_{\gamma+\varepsilon}} b_{\gamma+\varepsilon}$$

$$= \mathcal{D}_\gamma b_{\gamma-\varepsilon} - E_\gamma b_{\gamma+\varepsilon} \qquad \text{(B.12)}$$

in which we have defined

$$\mathcal{D}_\gamma = -\frac{D_\gamma}{c_{\gamma-\varepsilon}}, \quad E_\gamma = -\frac{E_\gamma}{c_{\gamma+\varepsilon}} \qquad \text{(B.13)}$$

provided that in (B.12) we ignore terms in which $c_{\gamma-\varepsilon} = 0$ (i.e., $n_{\gamma-\varepsilon} = 0$). Further, for both (B.7) and (B.13) we must stipulate that all terms calling for any $a_{\gamma-\varepsilon}$, $a_{\gamma+\varepsilon}$, $b_{\gamma-\varepsilon}$ or $b_{\gamma+\varepsilon}$ outside the range of the particular spectral truncation chosen must also be ignored.

Reference

Jahnke, E. and F. Emde, 1945: Tables of Functions. Dover, New York, 306 pp. plus tables.

Appendix C. Solution of a tridiagonal set of equations.

Suppose we have an equation set of the form

$$a_\gamma X_{\gamma-1} + b_\gamma X_\gamma + c_\gamma X_{\gamma+1} = R_\gamma$$
$$\gamma = 1, 2, 3, \ldots, \Gamma \tag{C.1}$$

where we must have

$$\left.\begin{aligned} a_1 &= 0 \\ c_\gamma &= 0 \end{aligned}\right\}. \tag{C.2}$$

That is, in matrix form we can write (C.1) as

$$AX = R \tag{C.3}$$

with A being tridiagonal of the form

$$A = \begin{bmatrix} b_1 & c_1 & \cdots & \cdots & 0 \\ a_2 & b_2 & c_2 & & \vdots \\ \vdots & \ddots & \ddots & \ddots & \vdots \\ & & a_\gamma & b_\gamma & c_\gamma \\ \vdots & & & \ddots & \ddots \\ 0 & \cdots & \cdots & a_\Gamma & b_\Gamma \end{bmatrix} \tag{C.4}$$

For solutions we define

$$\left.\begin{aligned} C_1 &= 1/b_1 \\ C_\gamma &= 1/(b_\gamma - a_\gamma c_{\gamma-1} C_{\gamma-1}); \quad 2 \le \gamma \le \Gamma \\ D_\gamma &= -c_\gamma C_\gamma \end{aligned}\right\} \tag{C.5}$$

and let

$$\left.\begin{aligned} B_1 &= C_1 R_1 \\ B_\gamma &= C_\gamma (R_\gamma - a_\gamma B_{\gamma-1}); \; 2 \leq \gamma \leq \Gamma \end{aligned}\right\}. \tag{C.6}$$

Then, the solutions appear as

$$\begin{aligned} X_\Gamma &= B_\Gamma \\ X_\gamma &= D_\gamma X_{\gamma+1} + B_\gamma; \; \gamma = \Gamma-1, \Gamma-2, \ldots, 1 \end{aligned} \tag{C.7}$$

provided all C_γ in (C.5) are finite. That is, if

$$\left.\begin{aligned} b_1 &\neq 0 \\ b_\gamma &\neq a_\gamma c_{\gamma-1} C_{\gamma-1} \end{aligned}\right\}. \tag{C.8}$$

Appendix D. Computation of the weight functions for Gaussian quadrature.

We consider the set of complete orthogonal Legendre polynomials, $P_n^{\ell}(\mu)$, in which $\ell = 0, \pm 1, \pm 2, \ldots$ and $n = 0, 1, 2, \ldots$. We define this set, according to (7.8), to be normalized such that

$$\int_{-1}^{1} P_n^{\ell}(\mu) P_{n'}^{\ell}(\mu) d\mu = 2\delta_{n,n'} \tag{D.1}$$

where μ is the sine of latitude or equivalently, the cosine of colatitude, ϕ. Now in order to expand an arbitrary function of latitude, say $f(\mu)$, in terms of the set of Legendre polynomials we let

$$f(\mu) = \sum_{\ell} \sum_{n} f_n^{\ell} P_n^{\ell}(\mu) \tag{D.2}$$

from which the coefficients, f_n^{ℓ}, are obtained through application of (D.1) such that

$$f_n^{\ell} = \frac{1}{2} \sum_{\ell} \sum_{n} f_{n'}^{\ell} \int_{-1}^{1} P_{n'}^{\ell}(\mu) P_n^{\ell}(\mu) d\mu = \frac{1}{2} \int_{-1}^{1} f(\mu) P_n^{\ell}(\mu) d\mu \ . \tag{D.3}$$

However, to be able to transform at will between spectral and grid point space, it is necessary to represent $f(\mu)$ at a number of discrete points, μ_k, in which $k = 1, 2, 3, \ldots, N$ with N being the total number of points lying within $-1<\mu<1$. Thus at each latitude point, (D.2) becomes

$$f(\mu_k) = \sum_{\ell} \sum_{n} f_n^{\ell} P_n^{\ell}(\mu_k) \ . \tag{D.4}$$

This means that in order to determine coefficients f_n^{ℓ} we must evaluate the inte-

grals in (D.3) numerically and at the same time maintain the orthogonality properties of the discrete polynomials representation in (D.4). For this purpose, integrating by quadratures, we introduce a set of Gaussian weight functions, w_k, such that

$$\sum_{k=1}^{N} w_k P_n^{\ell}(\mu_k) P_{n'}^{\ell}(\mu_k) \equiv \int_{-1}^{1} P_n^{\ell}(\mu) P_{n'}^{\ell}(\mu) d\mu \tag{D.5}$$

and the numerical analog for (D.3) becomes

$$\begin{aligned} f_n^{\ell} &= \frac{1}{2} \sum_{\ell} \sum_{n} f_{n'}^{\ell} \sum_{k=1}^{N} w_k P_{n'}^{\ell}(\mu_k) P_n^{\ell}(\mu_k) \\ &= \frac{1}{2} \sum_{k=1}^{N} w_k f(\mu_k) P_n^{\ell}(\mu_k) \quad . \end{aligned} \tag{D.6}$$

The remainder of this Appendix is devoted to the method of evaluation of the Gaussian weights, w_k.

Because we know that any given Legendre polynomial, $P_n^{\ell}(\mu)$, can be represented by a finite series in μ of at most degree n, we can expand

$$\left.\begin{aligned} P_n^{\ell}(\mu) P_{n'}^{\ell}(\mu) &= \sum_{i=0}^{n+n'} b_i \mu^i \\ \text{or} \qquad P_n^{\ell}(\mu_k) P_{n'}^{\ell}(\mu_k) &= \sum_{i=0}^{n+n'} b_i [\mu_k]^i \end{aligned}\right\} \tag{D.7}$$

and thus,

$$\int_{-1}^{1} P_n^{\ell}(\mu) P_{n'}^{\ell}(\mu) d\mu = \sum_{i=0}^{n+n'} b_i \int_{-1}^{1} \mu^i d\mu \quad . \tag{D.8}$$

Integrating (D.8) by quadratures using (D.5),

$$\int_{-1}^{1} P_n^{\ell}(\mu) P_{n'}^{\ell}(\mu) d\mu = \sum_{k=1}^{N} w_k P_n^{\ell}(\mu_k) P_{n'}^{\ell}(\mu_k)$$

$$= \sum_{k=1}^{N} w_k \sum_{i=0}^{n+n'} b_i [\mu_k]^i \quad . \tag{D.9}$$

Equating (D.8) and (D.9) we have

$$\sum_{i=0}^{n+n'} b_i \int_{-1}^{1} \mu^i d\mu = \sum_{k=1}^{N} w_k \sum_{i=0}^{n+n'} b_i [\mu_k]^i \tag{D.10}$$

and thus for any i such that $0 \leq i \leq n + n'$ it must hold that

$$\int_{-1}^{1} \mu^i d\mu = \sum_{k=1}^{N} w_k [\mu_k]^i \quad . \tag{D.11}$$

We see from (D.11) that if we choose the number of latitude points, N, such that $N-1 = n+n'$ then utilizing all $i = 0, 1, 2, \ldots, n+n$ we can form a set of N equations containing N unknown quantities, w_k, for inversion. However, in terms of colatitude, ϕ, we can show that any $\cos j\phi$ (j is an integer) can be expanded in the form

$$\left.\begin{aligned} \cos j\phi &= \sum_{m=0}^{j/2} a_{2m} \mu^{2m} = a_j \mu^j + \sum_{m=0}^{(j/2)-1} a_{2m} \mu^{2m} \\ \text{and} \\ \cos j\phi_k &= a_j [\mu_k]^j + \sum_{m=0}^{(j/2)-1} a_{2m} [\mu_k]^{2m} \end{aligned}\right\} \quad . \tag{D.12}$$

Then, inserting (D.12) into (D.11),

$$\frac{1}{a_i}\int_{-1}^{1}\text{cosi}\phi d\mu - \frac{1}{a_i}\sum_{m=0}^{(i/2)-1} a_{2m}\int_{-1}^{1}\mu^{2m}d\mu =$$

$$= \frac{1}{a_i}\sum_{k=1}^{N} w_k \text{cosi}\phi_k - \frac{1}{a_i}\sum_{m=0}^{(i/2)-1} a_{2m}\sum_{k=1}^{N} w_k[\mu_k]^{2m} \qquad (D.13)$$

or

$$\sum_{k=1}^{N} w_k \text{cosi}\phi_k = \int_{-1}^{1}\text{cosi}\phi d\mu$$

$$= \int_{0}^{\pi}\text{cosi}\phi\ \sin\phi d\phi$$

$$= \begin{cases} 0 \text{ for i odd} \\ \dfrac{-2}{i^2-1} \text{ for i even} \\ i = 0, 1, 2, \ldots, n+n' \end{cases} , \qquad (D.14)$$

where we have made use of (D.11) to eliminate the second term on each side of (D.13). Again, as for (D.11), we see that if we take N-1 = n+n', we can invert (D.14) to obtain the Gaussian weights.

As an example, consider N=3 where we select ϕ_1=30°, ϕ_2=90°, and ϕ_3=150°. Then, from (D.14) we can construct the set (using i = 0, 1, 2)

$$\left\{\begin{array}{ccccccc} w_1 & + & w_2 & + & w_3 & = & 2 \\ \frac{\sqrt{3}}{2}w_1 & & & - & \frac{\sqrt{3}}{2}w_3 & = & 0 \\ \frac{1}{2}w_1 & - & w_2 & + & \frac{1}{2}w_3 & = & -2/3 \end{array}\right\} \qquad (D.15)$$

with solutions

$$\left.\begin{aligned} w_1 &= w_3 = 4/9 \\ w_2 &= 10/9 \end{aligned}\right\} . \qquad \text{(D.16)}$$

We note that the solutions (D.16) are symmetric in w_k about the equator. If we assume such symmetry a priori then all equations in (D.14) involving odd values of i become redundant and we can write (D.14) over the integration interval from $\phi = 0$ to $\phi = \pi/2$ as

$$\left.\begin{aligned} \sum_{k=1}^{\frac{N+1}{2}} w_k \cos 2i\phi_k &= \int_0^{\pi/2} \cos 2i\phi \, \sin\phi \, d\phi \\ &= -\frac{1}{4i^2-1} ; \\ i &= 0, 1, 2, \ldots, \frac{n+n'}{2} \; ; \; N-1 = n+n' \end{aligned}\right\} . \qquad \text{(D.17)}$$

Again, using the example used above in which N=3, $\phi_1 = 30°$, and $\phi_2 = 90°$, we have $\frac{N+1}{2} = 2$ and $\frac{N-1}{2} = 1$ giving the set

$$\left\{\begin{aligned} w_1 + w_2 &= 1 \\ \tfrac{1}{2} w_1 - w_2 &= -\tfrac{1}{3} \end{aligned}\right\}$$

with solutions

$$\left.\begin{aligned} w_1 &= \frac{4}{9} \\ w_2 &= \frac{5}{9} \end{aligned}\right\} . \qquad \text{(D.18)}$$

Furthermore, if we want to obtain w_k's for the entire pole to pole integration, we need only make use of the symmetry property

$$W_{N+1-k} = w_k + \delta_{\phi_k,\pi/2}\, w_k \tag{D.19}$$

which gives for our example

$$\left.\begin{aligned} w_1 &= w_3 = \frac{4}{9} \\ w_2 &= \frac{5}{9} + \frac{5}{9} = \frac{10}{9} \end{aligned}\right\} . \tag{D.20}$$

Solutions (D.20) are identical with those of (D.16).

Appendix E. Transform methodology.

The transform routines take advantage of a number of factors related to the particular configuration of our model which allows for a considerable improvement in speed and efficiency. For example, since the physical fields that are being represented in our model are all real quantities (as opposed to complex values), we can make use of the inherent complex nature of Fourier transform theory to transform two of our fields simultaneously. Further savings in computational resources are possible by taking advantage of the odd/even nature of the Legendre polynomial expansions with latitude about the equator.

Consider the series representation

$$\psi(\lambda,\mu) = \sum_{\alpha} \psi_{\alpha} e^{i\ell_{\alpha}\lambda} P_{\alpha}(\mu) \tag{E.1}$$

in which we want to be able to transform freely between spatial data as represented by $\psi(\lambda,\mu)$ in (E.1) and coefficient data as determined by the $\{\psi_{\alpha}\}$ for a given truncation.

Now, in terms of even and odd series (with respect to the equator), we can write

$$\psi(\lambda,\mu) = \sum_{\alpha=\text{even}} \psi_{\alpha} e^{i\ell_{\alpha}\lambda} P_{\alpha}(\mu) + \sum_{\alpha=\text{odd}} \psi_{\alpha} e^{i\ell_{\alpha}\lambda} P_{\alpha}(\mu). \tag{E.2}$$

For simplicity we define

$$\left.\begin{aligned} E_{\ell}(\mu) &= \sum_{n_{\alpha}} \psi_{n_{\alpha}}^{\ell_{\alpha}} P_{n_{\alpha}}^{\ell_{\alpha}}(\mu) \;\; ; \; \alpha = \text{even} \\ O_{\ell}(\mu) &= \sum_{n_{\alpha}} \psi_{n_{\alpha}}^{\ell_{\alpha}} P_{n_{\alpha}}^{\ell_{\alpha}}(\mu) \;\; ; \; \alpha = \text{odd} \end{aligned}\right\} \tag{E.3}$$

where then $E_{\ell}(\mu)$ is even and $O_{\ell}(\mu)$ is odd (with respect to the equator). Thus,

for $\mu \geq 0$,

$$\left.\begin{aligned} \psi(\lambda,\mu) &= \sum_{\ell} [E_\ell(\mu) + O_\ell(\mu)]\, e^{i\ell\lambda} \\ \psi(\lambda,-\mu) &= \sum_{\ell} [E_\ell(\mu) - O_\ell(\mu)]\, e^{i\ell\lambda} \end{aligned}\right\} \quad (E.4)$$

We now let (for $\mu \geq 0$)

$$\left.\begin{aligned} A_\ell(\mu) &= (1+i)\, E_\ell(\mu) + (1-i)\, O_\ell(\mu) \\ B_\ell(\mu) &= (1+i)\, E^*_\ell(\mu) + (1-i)\, O^*_\ell(\mu) \end{aligned}\right\} \quad (E.5)$$

in which "*" denotes complex conjugation. We then can write

$$\left.\begin{aligned} A(\lambda,\mu) &= \psi(\lambda,\mu) + i\psi(\lambda,-\mu) \\ &= \sum_{\ell}[(1+i)E_\ell(\mu) + (1-i)O_\ell(\mu)]\, e^{i\ell\lambda} \\ &= \sum_{\ell} A_\ell(\mu)\, e^{i\ell\lambda} \\ B(\lambda,\mu) &= \psi(\lambda,\mu) - i\psi(\lambda,-\mu) \\ &= \sum_{\ell}[(1-i)E_\ell(\mu) + (1+i)O_\ell(\mu)]\, e^{i\ell\lambda} \\ &= \sum_{\ell} B^*_\ell(\mu)\, e^{i\ell\lambda} \end{aligned}\right\} \quad (E.6)$$

Using the definitions and relationships developed above, we now turn to a description of the computational routines developed for the spectral to grid and grid to spectral transformations required in the model.

I. Spectral to grid transformations

a. Subroutine SPCGD2 (DSPEC, DATA)

This routine transforms spectral coefficients (stored in "DSPEC") to grid values ("DATA") at the Gaussian latitudes.

The routine calls subroutines "SPFOR2" and "FFTFR2".

Storage locations for the input coefficient matrix "DSPEC" and the output grid point matrix "DATA" are illustrated below.

1. Storage arrangement for "DSPEC". Assume a matrix of complex spectral coefficients, ψ_α, in which the vector index "α" is as defined, for example, as in Appendix A (A-2). The index "NLEV" represents the total number of model levels. Then,

I \ J	1 (LEVEL 1) . . . . . NLEV (LEVEL NLEV)	33 (LEVEL 1) . . . . . 32 + NLEV (LEVEL NLEV)
1.	$Re\{\psi_1\}$ . . . . . $Re\{\psi_1\}$	$Im\{\psi_1\}$ . . . . . $Im\{\psi_1\}$
2.	$Re\{\psi_2\}$ . . . . . $Re\{\psi_2\}$	$Im\{\psi_2\}$ . . . . . $Im\{\psi_2\}$
.	. .	. .
.	. .	. .
.	. .	. .
.	. .	. .
.	. .	. .
α_{MAX}	$Re\{\psi_{\alpha_{MAX}}\}$ . . . . . $Re\{\psi_{\alpha_{MAX}}\}$	$Im\{\psi_{\alpha_{MAX}}\}$ . . . . . $Im\{\psi_{\alpha_{MAX}}\}$

2. Storage arrangement for "DATA". Assume ψ now represents elements in a matrix of real gridpoint values. Here "NLON" and "NGRID" are, for a given model level, the number of longitude points along a given latitude circle and the total number of gridpoints, respec-

tively. Note that data for the conjugate (i.e., Southern Hemisphere) latitudes appear in the last 32 columns of the matrix. Thus,

I \ J	1 (LEVEL 1)	. . . . .	NLEV (LEVEL NLEV)	33 (LEVEL 1)	. . . . .	32 + NLEV (LEVEL NLEV)
1	$\psi(\lambda_1,\mu_1)$	. . .	$\psi(\lambda_1,\mu_1)$	$\psi(\lambda_1,-\mu_1)$	. . .	$\psi(\lambda_1,-\mu_1)$
2	$\psi(\lambda_2,\mu_1)$	. . .	$\psi(\lambda_2,\mu_1)$	$\psi(\lambda_2,-\mu_1)$	. . .	$\psi(\lambda_2,-\mu_1)$
	. . .		. . .	. . .		. . .
NLON	$\psi(\lambda_{NLON},\mu_1)$	. . .	$\psi(\lambda_{NLON},\mu_1)$	$\psi(\lambda_{NLON},-\mu_1)$	. . .	$\psi(\lambda_{NLON},-\mu_1)$
NLON+1	$\psi(\lambda_1,\mu_2)$	. . .	$\psi(\lambda_1,\mu_2)$	$\psi(\lambda_1,-\mu_2)$	. . .	$\psi(\lambda_1,-\mu_2)$
NLON+2	$\psi(\lambda_2,\mu_2)$	. . .	$\psi(\lambda_2,\mu_2)$	$\psi(\lambda_2,-\mu_2)$	. . .	$\psi(\lambda_2,-\mu_2)$
	. . .		. . .	. . .		. . .
2*NLON	$\psi(\lambda_{NLON},\mu_2)$	. . .	$\psi(\lambda_{NLON},\mu_2)$	$\psi(\lambda_{NLON},-\mu_2)$	. . .	$\psi(\lambda_{NLON},-\mu_2)$
2*NLON+1	$\psi(\lambda_1,\mu_3)$	. . .	$\psi(\lambda_1,\mu_3)$	$\psi(\lambda_1,-\mu_3)$	. . .	$\psi(\lambda_1,-\mu_3)$
	. . .		. . .	. . .		. . .
NGRID/2	$\psi(\lambda_{NLON},\mu_{EQ})$	. . .	$\psi(\lambda_{NLON},\mu_{EQ})$	$\psi(\lambda_{NLON},-\mu_{EQ})$	. . .	$\psi(\lambda_{NLON},-\mu_{EQ})$

b. Subroutine SPFOR2 (DSPEC, DATA)

This routine determines Fourier coefficients (returned in "DATA") for each latitude using the spectral coefficients in "DSPEC".

1. "DSPEC" is the input coefficient field as in subroutine "SPCGD2".
2. The complex Fourier coefficient output is returned in "DATA" in a

form which combines the conjugate latitude values. Thus, "DATA" will contain the $A_\ell(\mu)$ and $B_\ell(\mu)$ fields defined in (E.5) as re-required for the grid value expansions of (E.6). In the following matrix table, L_{MAX} is the maximum planetary (or longitudinal) wave number, LR1 = L_{MAX}+1, and "NLAT" is the number of Gaussian latitudes. All other quantities have been defined previously. The storage arrangement for A_ℓ and B_ℓ is as follows:

(See following page).

I \ J	1 (LEVEL 1)	. . . .	NLEV (LEVEL NLEV)	33 (LEVEL 1)	. . . .	32 + NLEV (LEVEL NLEV)
1	$Re\{A_0(\mu_1)\}$	. . .	$Re\{A_0(\mu_1)\}$	$Im\{A_0(\mu_1)\}$	. . .	$Im\{A_0(\mu_1)\}$
2	$Re\{A_1(\mu_1)\}$	. . .	$Re\{A_1(\mu_1)\}$	$Im\{A_1(\mu_1)\}$	. . .	$Im\{A_1(\mu_1)\}$
	.		.	.		.
	.		.	.		.
	.		.	.		.
LR1	$Re\{A_{L_{MAX}}(\mu_1)\}$	. . .	$Re\{A_{L_{MAX}}(\mu_1)\}$	$Im\{A_{L_{MAX}}(\mu_1)\}$	. . .	$Im\{A_{L_{MAX}}(\mu_1)\}$
LR1+1	0	. . .	0	0	. . .	0
	.		.	.		.
	.		.	.		.
	.		.	.		.
NLON-L_{MAX}	0	. . .	0	0	. . .	0
NLON-L_{MAX+1}	$Re\{B_{L_{MAX}}(\mu_1)\}$	. . .	$Re\{B_{L_{MAX}}(\mu_1)\}$	$Im\{B_{L_{MAX}}(\mu_1)\}$	. . .	$Im\{B_{L_{MAX}}(\mu_1)\}$
	.		.	.		.
	.		.	.		.
	.		.	.		.
NLON-1	$Re\{B_2(\mu_1)\}$	. . .	$Re\{B_2(\mu_1)\}$	$Im\{B_2(\mu_1)\}$	. . .	$Im\{B_2(\mu_1)\}$
NLON	$Re\{B_1(\mu_1)\}$	. . .	$Re\{B_1(\mu_1)\}$	$Im\{B_1(\mu_1)\}$	. . .	$Im\{B_1(\mu_1)\}$
NLON+1	$Re\{A_0(\mu_2)\}$	. . .	$Re\{A_0(\mu_2)\}$	$Im\{A_0(\mu_2)\}$	. . .	$Im\{A_0(\mu_2)\}$
NLON+2	$Re\{A_1(\mu_2)\}$	. . .	$Re\{A_1(\mu_2)\}$	$Im\{A_1(\mu_2)\}$	. . .	$Im\{A_1(\mu_2)\}$
	.		.	.		.
	.		.	.		.
	.		.	.		.
2*NLON	$Re\{B_1(\mu_2)\}$	. . .	$Re\{B_1(\mu_2)\}$	$Im\{B_1(\mu_2)\}$	. . .	$Im\{B_1(\mu_2)\}$
	.		.	.		.
	.		.	.		.
	.		.	.		.
	.		.	.		.
NLAT/2*NLON	$Re\{B_1(\mu_{EQ})\}$	. . .	$Re\{B_1(\mu_{EQ})\}$	$Im\{B_1(\mu_{EQ})\}$	. . .	$Im\{B_1(\mu_{EQ})\}$

c. Subroutine FFTFR2 (DATA)

This routine converts the Fourier coefficients obtained in "DATA" from "SPCFR2" to grid values (also stored in "DATA"), as described for subroutine "SPCGD2", using fast Fourier transform (FFT) techniques. The transformation can be reversed by changing the sign on the flag variable, "ISIGN". It thus is used as the first step in transforming grid data to full spectral coefficient data.

II. Grid to spectral transformations.

a. Subroutine GDSPC2 (DSPEC, DATA).

This routine reverses the procedure of "SPCGD2" and produces spectral output in "DSPEC" from gridpoint data contained in "DATA". The storage arrangements for these two fields are as described in "SPCGD2". The program begins by moving one latitude (and its congugate latitude) of data from "DATA" to "DSPEC" on a temporary basis and then calling subroutine FFTFT2 (DSPEC) with argument "DSPEC" in order to compute the A_ℓ and B_ℓ fields for that latitude.

b. "GDSPC2" then continues by combining the $A_\ell(\mu)$ and $B_\ell(\mu)$ fields (again, by latitudes) to obtain fields of $E_\ell(\mu)$ and $O_\ell(\mu)$ as defined in (E.3). These are given (for $\ell > 0$) by

$$\left.\begin{aligned} E_\ell(\mu) &= \tfrac{1}{4}[A_\ell(\mu)+B^*_\ell(\mu)] + \tfrac{i}{4}[A_\ell(\mu)-B^*_\ell(\mu)] \\ O_\ell(\mu) &= \tfrac{1}{4}[A_\ell(\mu)+B^*_\ell(\mu)] - \tfrac{i}{4}[A_\ell(\mu)-B^*_\ell(\mu)] \end{aligned}\right\} \quad (E.7)$$

and, for $\ell = 0$,

$$\left.\begin{aligned} E_0(\mu) &= \tfrac{1}{2}[Re\{A_0(\mu)\} + Im\{A_0(\mu)\}] \\ O_0(\mu) &= \tfrac{1}{2}[Re\{A_0(\mu)\} - Im\{A_0(\mu)\}] \end{aligned}\right\} \quad (E.8)$$

where $E_0(\mu)$ and $O_0(\mu)$ are both real quantities. Due to limitations in

storage, however, the $E_\ell(\mu)$ and $O_\ell(\mu)$ values are stored both in the "DSPEC" and "DATA" matrices. That is, it was found to be convenient to place the E_ℓ and O_ℓ coefficients for the first three planetary waves (ℓ = 0, 1, and 2) in the region DSPEC(1,107) - DSPEC(64,190). All of the other coefficients ($\ell \geq 3$) are placed in "DATA" by latitudes. The storage arrangements for both "DSPEC" and "DATA" follow. First, however, we want to note, for ease of computation, that we can make use of the definition, for example,

$$A^{\dagger} = Im\{A\} + iRe\{A\} \tag{E.9}$$

so that (E.7) can be written as

$$\left.\begin{aligned} E_\ell(\mu) &= .25\ [A_\ell(\mu)+B^*_\ell(\mu)+(A^*_\ell(\mu)-B_\ell(\mu))^{\dagger}] \\ O_\ell(\mu) &= .25\ [A_\ell(\mu)+B^*_\ell(\mu)-(A^*_\ell(\mu)-B_\ell(\mu))^{\dagger}] \end{aligned}\right\} \tag{E.10}$$

Define, NLATHF = (NLAT+1)/2 and J2 = NLATHF+NLATHF such that the storage for "DSPEC" is:

(See following page).

I \ J	1 (LEVEL 1)	. . . .	NLEV (LEVEL NLEV)	33 (LEVEL 1)	. . . .	32 + NLEV (LEVEL NLEV)
1						
2						
.						
.						
.						
106						
107	$Re\{E_0(\mu_1)\}$	. . .	$Re\{E_0(\mu_1)\}$	0	. . .	0
108	$Re\{O_0(\mu_1)\}$	. . .	$Re\{O_0(\mu_1)\}$	0	. . .	0
109	$Re\{E_0(\mu_2)\}$	. . .	$Re\{E_0(\mu_2)\}$	0	. . .	0
110	$Re\{O_0(\mu_2)\}$	. . .	$Re\{O_0(\mu_2)\}$	0	. . .	0
	.		.	.		.
	.		.	.		.
	.		.	.		.
105+J2	$Re\{E_0(\mu_{EQ})\}$	. . .	$Re\{E_0(\mu_{EQ})\}$	0	. . .	0
106+J2	$Re\{O_0(\mu_{EQ})\}$	. . .	$Re\{O_0(\mu_{EQ})\}$	0	. . .	0
107+J2	$Re\{E_1(\mu_1)\}$	. . .	$Re\{E_1(\mu_1)\}$	$Im\{E_1(\mu_1)\}$	. . .	$Im\{E_1(\mu_1)\}$
108+J2	$Re\{O_1(\mu_1)\}$	. . .	$Re\{O_1(\mu_1)\}$	$Im\{O_1(\mu_1)\}$	. . .	$Im\{O_1(\mu_1)\}$
	.		.	.		.
	.		.	.		.
	.		.	.		.
106+2*J2	$Re\{O_1(\mu_{EQ})\}$	. . .	$Re\{O_1(\mu_{EQ})\}$	$Im\{O_1(\mu_{EQ})\}$	. . .	$Im\{O_1(\mu_{EQ})\}$
107+2*J2	$Re\{E_2(\mu_1)\}$	. . .	$Re\{E_2(\mu_1)\}$	$Im\{E_2(\mu_1)\}$	. . .	$Im\{E_2(\mu_1)\}$
	.		.	.		.
	.		.	.		.
	.		.	.		.
106+3*J2	$Re\{O_2(\mu_{EQ})\}$	. . .	$Re\{O_2(\mu_{EQ})\}$	$Im\{O_2(\mu_{EQ})\}$	. . .	$Im\{O_2(\mu_{EQ})\}$

C-2

For "DATA" we let J2 = 2*NLATHF*(L_{MAX}-3) where then:

I \ J	1 (LEVEL 1)	. . .	NLEV (LEVEL NLEV)	33 (LEVEL 1)	. . .	32 + NLEV (LEVEL NLEV)
1	$Re\{E_3(\mu_1)\}$	. . .	$Re\{E_3(\mu_1)\}$	$Im\{E_3(\mu_1)\}$	. . .	$Im\{E_3(\mu_1)\}$
2	$Re\{O_3(\mu_1)\}$	. . .	$Re\{O_3(\mu_1)\}$	$Im\{O_3(\mu_1)\}$	. . .	$Im\{O_3(\mu_1)\}$
3	$Re\{E_4(\mu_1)\}$	. . .	$Re\{E_4(\mu_1)\}$	$Im\{E_4(\mu_1)\}$	. . .	$Im\{E_4(\mu_1)\}$
4	$Re\{O_4(\mu_1)\}$	. . .	$Re\{O_4(\mu_1)\}$	$Im\{O_4(\mu_1)\}$	. . .	$Im\{O_4(\mu_1)\}$
	.		.	.		.
	.		.	.		.
	.		.	.		.
$2*L_{MAX}-7$	$Re\{E_{L_{MAX}}(\mu_1)\}$	. . .	$Re\{E_{L_{MAX}}(\mu_1)\}$	$Im\{E_{L_{MAX}}(\mu_1)\}$	. . .	$Im\{E_{L_{MAX}}(\mu_1)\}$
$2*L_{MAX}-6$	$Re\{O_{L_{MAX}}(\mu_1)\}$	. . .	$Re\{O_{L_{MAX}}(\mu_1)\}$	$Im\{O_{L_{MAX}}(\mu_1)\}$	. . .	$Im\{O_{L_{MAX}}(\mu_1)\}$
$2*L_{MAX}-5$	$Re\{E_3(\mu_2)\}$	. . .	$Re\{E_3(\mu_2)\}$	$Im\{E_3(\mu_2)\}$	. . .	$Im\{E_3(\mu_2)\}$
$2*L_{MAX}-4$	$Re\{O_3(\mu_2)\}$	. . .	$Re\{O_3(\mu_2)\}$	$Im\{O_3(\mu_2)\}$	. . .	$Im\{O_3(\mu_2)\}$
	.		.	.		.
	.		.	.		.
	.		.	.		.
$4*L_{MAX}-12$	$Re\{O_{L_{MAX}}(\mu_2)\}$	. . .	$Re\{O_{L_{MAX}}(\mu_2)\}$	$Im\{O_{L_{MAX}}(\mu_2)\}$	. . .	$Im\{O_{L_{MAX}}(\mu_2)\}$
	.		.	.		.
	.		.	.		.
	.		.	.		.
J2	$Re\{O_{L_{MAX}}(\mu_{EQ})\}$	. . .	$Re\{O_{L_{MAX}}(\mu_{EQ})\}$	$Im\{O_{L_{MAX}}(\mu_{EQ})\}$	. . .	$Im\{O_{L_{MAX}}(\mu_{EQ})\}$